SYNTHESIS OF SURFACE MODIFIED SILVER SULFIDE NANOPARTICLES AS ANTIFUNGAL AGENTS

Thesis

Submitted to the Punjab Agricultural University
in partial fulfilment of the requirements
for the degree of

MASTER OF SCIENCE
in
CHEMISTRY
(Minor Subject: Biochemistry)

By

GARIMA SETHI
(L-2017-BS-267-M)

Department of Chemistry
College of Basic Sciences and Humanities

LUDHIANA – 141004

2019

CERTIFICATE-I

This is to certify that the thesis entitled **"Synthesis of surface modified silver sulfide nanoparticles as antifungal agents"** submitted for the degree of **2-year M.Sc. Programme,** in the subject of **Chemistry** (Minor subject: **Biochemistry**) of the Punjab Agricultural University, Ludhiana, is a bonafide research work carried out by **Ms. Garima Sethi (L-2017-BS-267-M)** under my supervision and that no part of this thesis has been submitted for any other degree.

The assistance and help received during the course of investigation have been fully acknowledged.

_____

Dr. (Mrs.) Anjali
Major Advisor
Assistant Professor
Department of Chemistry
Punjab Agricultural University,
Ludhiana-141 004.

CERTIFICATE-II

This is to certify that the thesis entitled, **"Synthesis of surface modified silver sulfide nanoparticles as antifungal agents"** submitted by **Ms. Garima Sethi (L-2017-BS-267-M)** to the Punjab Agricultural University, Ludhiana, in partial fulfillment of the requirements for the degree of **2-year M.Sc. Programme,** in the subject of **Chemistry** (Minor subject: **Biochemistry**) has been approved by the Student's Advisory Committee along with External Examiner after an oral examination on the same.

_____
(Dr. (Mrs.) Anjali)
Major Advisor

_____
(Dr. Damanjit Singh)
External Examiner
Associate Professor
Department of Chemistry
Sant Longowal Institute of
Engineering and Technology
Sangrur

_____
(Dr. (Mrs.) Sucheta Sharma)
Head of the Department

_____
(Dr. (Mrs.) G.K. Sangha)
Dean, Postgraduate Studies

ACKNOWLEDGEMENT

Firstly, I bow my head with utmost reverence before the ***Almighty*** *whose eternal blessings has enabled me to accomplish this noble effort.*

It gives me immense pleasure to express my thanks and sense of profound gratitude to my Major Advisor ***Dr. (Mrs.) Anjali****, Assistant Professor, Department of Chemistry, Punjab Agricultural University, Ludhiana, for her expert guidance, encouragement, inspiration and advice throughout my research work. It was my privilege to be guided by a person of calibre, whose blessings bring best in every one of my endeavours.*

I owe my unpayable debt to the other esteemed members of the department and my advisory committee, Special thanks are accorded to ***Dr.(Mrs.) Manpreet Kaur,*** *Assistant Professor, Department of Chemistry,* ***Dr. (Mrs.) Ritu Tandon****, Assistant Chemist, Punjab Horticultural Postharvest Technology Centre,* ***Dr. (Mrs.) Anju Bala,*** *, Assistant Plant Pathologist ,Department of Plant Breeding and Genetics and* ***Dr. (Mrs.) Satvir Kaur,*** *Assistant Biochemist, Department of Biochemistry, for their able guidance , constructive suggestions and continuous support.*

I am indebted to my respected parents and express my profound gratitude to my father ***Mr. Varinder Sethi*** *and mother* ***Mrs. Renu Sethi*** *for their constant words of encouragement, deep affection and heartful blessings that enabled me to reach this stage of career. I am also thankful to* ***Aradhya and Rishad,*** *my younger siblings and my* ***grandparents*** *for helping me and encouraging me whenever needed.*

Friends are always a moral support which is extremely important when one is feeling low. I take great pleasure in thanking my friend ***Dr. Mohit kamboj*** *for his help, unconditional love and for being a wonderful company during my stay at PAU. I also thank my friends* ***Manpreet Kaur, Inderpal kaur, Riddhi, Divya, Taruna*** *and* ***Shifalli*** *for moral support and every possible help. A special word of appreciation for my labmates,* ***Dr. Amit Kumar, Radha, Shilpa, Heena, Varinder*** *and* ***Harmandeep*** *who created good working atmosphere in the laboratory. I am also obliged to be involved in the social cause of teaching that help me release my stress and give me the courage to buck up again.*

I also pay me sincerest thanks to all the other members of the department for their invaluable and generous help.

I feel proud to be a part of PAU, Ludhiana where I learnt a lot and spent some unforgettable memories of my life.

Date: _____

Place: ***Garima Sethi***

Title of the Dissertation	:	Synthesis of surface modified silver sulfide nanoparticles as antifungal agents
Name of the Student and Admission No.	:	Garima Sethi (L-2017-BS-267-M)
Major Subject	:	Chemistry
Minor Subject	:	Biochemistry
Name and Designation of Major Advisor	:	Dr. (Mrs.) Anjali Assistant Professor
Degree to be Awarded	:	M.Sc.
Year of Award of Degree	:	2019
Total Pages in Dissertation	:	61 + Annexure (i) + VITA
Name of University	:	Punjab Agricultural University, Ludhiana-141004

ABSTRACT

Nanoparticles have great potential in the fields of biomedicine, building materials, environmental protection, antibacterial and antifungal agents. Silver sulfide nanoparticles (Ag_2S NPs) have been synthesized for their applications in various fields including photoconductors, photovoltaic cells, solar selective coatings and infrared detectors, but have less reporting as bio-compatible material or in *in vitro* or *in vivo* applications. Silver sulfide has been hypothesized as less toxic form in nature as metal nanoparticles of soft nature get their ultimate fate by sulfidation as their natural pathway of detoxification. In this study we synthesized silver sulfide nanoforms by approaching sonochemical method. Various sulfide ion sources and silver nitrate were used as initial components for the synthesis of silver sulfide nanoparticles (Ag_2S NPs). All the synthesized samples were tested for their preliminary *in vitro* antifungal activity against *Ustilago hordei, Uromyces viciafabia*, *Fusarium moniliforme* and *Bipolaris oryzae* . Ag_2S-4 NPs synthesized from sodium sulfide showed better antifungal potential in comparsion to silver nanoparticles (Ag NPs) and commercially used standard fungicides. The Ag_2S-4 NPs sample was further coated with chitosan to get chitosan decorated silver sulfide nanoparticles to evaluate the antifungal potential of this conjugate in comparison to Ag_2S NPs.

Keywords Silver sulfide, nanoform, sonochemical irradiation, pathogenic fungi, chitosan

_____ _____

Signature of Major Advisor **Signature of the Student**

ਖੋਜ ਗ੍ਰੰਥ ਦਾ ਸਿਰਲੇਖ	:	ਸਤ੍ਹਾ ਸੋਧ ਸਿਲਵਰ ਸਲਫਾਈਡ ਨੈਨੋਪਾਰਟਿਕਲਸ ਦੀ ਐਂਟੀਫੰਗਲ ਏਜੰਟਾ ਦੇ ਤੌਰ ਤੇ ਸੰਸਲੇਸ਼ਣ
ਵਿਦਿਆਰਥੀ ਦਾ ਨਾਂ ਅਤੇ ਦਾਖ਼ਲਾ ਨੰਬਰ	:	ਗਰੀਮਾ ਸੇਠੀ (ਐੱਲ-2017-ਬੀ.ਐੱਸ-267-ਐੱਮ)
ਮੁੱਖ ਵਿਸ਼ਾ	:	ਰਸਾਇਣ ਵਿਗਿਆਨ
ਸਹਿਯੋਗੀ ਵਿਸ਼ਾ	:	ਜੀਵ-ਰਸਾਇਣ ਵਿਗਿਆਨ
ਮੁੱਖ ਸਲਾਹਕਾਰ ਦਾ ਨਾਂ ਅਤੇ ਅਹੁੱਦਾ	:	ਡਾ. ਅੰਜਲੀ ਅਸਿਸਟੈਂਟ ਪ੍ਰੋਫੈਸਰ
ਡਿਗਰੀ	:	ਮਾਸਟਰ ਆਫ਼ ਸਾਇੰਸ
ਡਿਗਰੀ ਨਾਲ ਸਨਮਾਨਿਤ ਕਰਨ ਦਾ ਸਾਲ	:	2019
ਖੋਜ਼ ਪੱਤਰ ਵਿਚ ਕੁੱਲ ਪੰਨੇ	:	61 + ਅੰਤਿਕਾ (i) + ਵੀਟਾ
ਯੂਨੀਵਰਸਿਟੀ ਦਾ ਨਾਮ	:	ਪੰਜਾਬ ਖੇਤੀਬਾੜੀ ਯੂਨੀਵਰਸਿਟੀ, ਲੁਧਿਆਣਾ- 141004, ਪੰਜਾਬ, ਭਾਰਤ ।

ਸਾਰ-ਅੰਸ਼

ਬਾਇਓਮੈਡਿਸੀਨ, ਬਿਲਡਿੰਗ ਸਾਮੱਗਰੀ, ਵਾਤਾਵਰਣ ਸੁਰੱਖਿਆ, ਐਂਟੀਬੈਕਟੀਰੀਅਲ ਅਤੇ ਐਂਟੀਫੰਗਲ ਏਜੰਟ ਦੇ ਖੇਤਰਾਂ ਵਿੱਚ ਨੈਨੋਪਾਰਟਿਕਲਸ ਦੀ ਬਹੁਤ ਸਮਰੱਥਾ ਹੈ। ਸਿਲਵਰ ਸਲਫਾਈਡ ਨੈਨੋਪਾਰਟਿਕਲਸ ਨੂੰ ਉਨ੍ਹਾਂ ਦੇ ਕਾਰਜਾਂ ਲਈ ਫੋਟੋ- ਕੰਨਡਕਟਰਾਂ, ਫੋਟੋਵੋਲਟੇਏਕ ਕੋਸ਼ੀਕਾਵਾਂ, ਸੂਰਜੀ ਚਣਾਲੀ ਕੋਟਿੰਗ ਅਤੇ ਇਨਫਰਾਰੈੱਡ ਡਿਟੇਕਟਰਾਂ ਸਮੇਤ ਵੱਖ-ਵੱਖ ਖੇਤਰਾਂ ਵਿੱਚ ਤਿਆਰ ਕੀਤਾ ਗਿਆ ਹੈ, ਲੇਕਿਨ ਬਾਇਓ-ਅਨੁਕੂਲ ਸਾਮੱਗਰੀ ਜਾਂ ਇਨਵਿਟਰੋ ਜਾਂ ਵੀਵੋ ਐਪਲੀਕੇਸ਼ਨਾਂ ਵਿੱਚ ਘੱਟ ਰਿਪੋਰਟਿੰਗ ਹੈ। ਸਿਲਵਰ ਸਲਫਾਈਡ ਨੂੰ ਪ੍ਰਭਾਵੀ ਘੱਟ ਜ਼ਹਿਰੀਲੇ ਰੂਪ ਦੇ ਤੌਰ ਤੇ ਪ੍ਰਭਾਸ਼ਿਤ ਕੀਤਾ ਗਿਆ ਹੈ, ਕਿਉਂਕਿ ਨਰਮ ਸੁਭਾਅ ਦੇ ਧਾਤ ਨੂੰ ਨੈਨੋਪੈਕਟਿਕਲਸ ਸਲਫਾਈਡੇਸ਼ਨ ਦੁਆਰਾ ਆਪਣੇ ਅਖੀਰਲੀ ਕਿਸਮਤ ਨੂੰ ਨਿਕੰਮੀਕਰਨ ਦੇ ਕੁਦਰਤੀ ਮਾਰਗ ਵਜੋਂ ਪ੍ਰਾਪਤ ਕਰਦੇ ਹਨ। ਇਸ ਅਧਿਐਨ ਵਿੱਚ ਅਸੀਂ ਸੋਨਾਕੈਮੀਕਲ ਵਿਧੀ ਦੀ ਵਰਤੋਂ ਦੁਆਰਾ ਸਿਲਵਰ ਸਲਫਾਇਡ ਨੈਨੋਫਾਰਮ ਨੂੰ ਬਣਾਇਆ। ਕਈ ਸਲਫਾਇਡ ਆਇਨ ਸਰੋਤ ਅਤੇ ਸਿਲਵਰ ਨਾਈਟ੍ਰੇਟ ਨੂੰ ਸਿਲਵਰ ਸਲੱਫਾਈਡ ਨੈਨੋਪਾਰਟਿਕਲਸ ਦੇ ਸੰਸਲੇਸ਼ਣ ਲਈ ਸ਼ੁਰੂਆਤੀ ਭਾਗਾਂ ਵਜੋਂ ਵਰਤਿਆ ਗਿਆ ਸੀ। ਸਭ ਸੰਮਲੇਨਿਤ ਨਮੂਨਿਆਂ ਨੂੰ ਚਾਰ ਟੈਸਟ ਉੱਲੀਆਂ (ਅਸਟਿਲਗੋ ਹੌਰਡੀਆਈ, ਯੂਰੋਮੀਸਿਸ ਵਿਸੀਆਫੈਬਿਆ, ਫਿਊਸਰੀਅਮ ਮੋਨਿਲਿਫਰਮਿ ਅਤੇ ਬਾਇਪੋਲਰਿਸ ਔਰੀਜ਼ਾ) ਐਂਟੀਫੰਗਲ ਸਰਗਰਮੀ ਲਈ ਮੁਲਾਂਕਣ ਕੀਤਾ ਗਿਆ। ਇਸ ਅਧਿਐਨ ਦੌਰਾਨ ਸੋਡੀਅਮ ਸਲਫਾਇਡ ਦੁਆਰਾ ਸੰਚਿਤਿਤ ਗਿਆ ਕੀਤਾ ਨਮੂਨਾ (Ag_2S-4 NPs) ਬਾਕੀ ਸਾਰੇ ਨਮੂਨਿਆਂ ਅਤੇ ਵਪਾਰਕ ਤੌਰ ਤੇ ਵਰਤੇ ਜਾਣ ਵਾਲੇ ਫਨਜੀਸਾਈਡਜ਼ ਤੋਂ ਵੱਧ ਅਸਰਦਾਰ ਐਂਟੀਫੰਗਲ ਏਜੰਟ ਸੀ। ਸਭ ਤੋਂ ਵੱਧ ਐਂਟੀਫੰਜਲ ਸਮਰੱਥਾ ਰੱਖਣ ਵਾਲੇ Ag_2S-4 NPs ਨੂੰ ਕਾਈਟੋਸਨ ਨਾਲ ਜੋੜਿਆ ਗਿਆ ਅਤੇ ਇਸ ਦੀ ਤੁਲਨਾ ਸਿਲਵਰ ਸਲਫਾਇਡ ਨੈਨੋਪਾਰਟਿਕਲਸ ਨਾਲ ਕੀਤੀ ਗਈ ਸੀ ।

ਮੁੱਖ ਸ਼ਬਦ: ਸਿਲਵਰ ਸਲਫਾਈਡ, ਨੈਨੋਫਾਰਮ, ਸੋਨਾਕੈਮੀਕਲ ਵਿਧੀ, ਐਂਟੀਫੰਗਲ, ਕਾਈਟੋਸਨ

_____ _____

ਮੁੱਖ ਸਲਾਹਕਾਰ ਦੇ ਹਸਤਾਖਰ **ਵਿੱਦਿਆਰਥੀ ਦੇ ਹਸਤਾਖਰ**

CONTENTS

LIST OF TABLES

LIST OF FIGURES

CHAPTER-I

INTRODUCTION

Nanostructured materials have attained a great deal of interest in the last few years for their fascinating physical properties, chemical properties, topo-morphological and hence bio-potential (Nath and Kalita 2012). Increasing number of published research papers show great interest of scientists for the importance of metal nanoparticles (M NPs) and engineered metal nanoparticles (ENPs) for their wider applications. M NPs of transition metals are generally soft natured, which get their ultimate fate by sulfidation as their natural pathway of detoxification (Wang *et al* 2013), i.e. metal sulfides are most detoxified form of M NPs.

Metal sulfides nanoparticles (MS NPs) have less exploitation on bioapplication scenario. Nanotoxicity is an important aspect which is needed to be addressed before going for *in vitro* activities. Soft metal sulfides are the stable chemical form and therefore are hypothesized as most detoxified form of M NPs (Sidhu *et al* 2017). MS NPs of various metals such as silver (Ag), iron (Fe), zinc (Zn), cadmium (Cd), manganese (Mn) and copper (Cu) etc., have been reported in terms of synthesis with varied nano morphologies. Metal sulfides of transition metals are water insoluble and their nano dispersion in water makes them more appropriate in terms of application (Guo *et al* 2013), in finding new agrochemicals. Modifications as aqua formulations of insoluble materials (Sidhu *et al* 2017) are the essence of applied bio nanotechnological applications.

Silver nanoparticles (Ag NPs) have wide applications and have been commercialized in various ways (Tran *et al* 2013). Silver has been used as an antimicrobial agent since ancient civilizations (Ebrahiminezhad *et al* 2016). Use of silver nanoparticles, as an alternative to chemical pesticides and antimicrobial agents has become common. Mishra *et al* (2014) reported AgNPs active against *Serratia* sp. and *Bipolaris sorokiniana*. Krishnaraj *et al* (2012) conducted *in vitro* assays and reported biosynthesized silver nanoparticles, which act as a strong inhibitory agent against various fungal diseases. The infectious diseases caused by *Bipolaris sorokiniana* in wheat plants was effectively controlled by green biologically synthesized silver nanoparticles and exhibited strong antifungal activity against it (Mishra *et al* 2014). Silver sulfide nanoparticles (Ag_2S NPs) reported for antimicrobial evaluation inflicted a growth inhibition of more than 75% against *E. coli* (ATCC 13534), *E. coli* (ATCC 25922) and *Staphylococcus aureus* (ATCC 25923) (Kumari *et al* 2014) along with appreciable antioxidant activities (Kumar *et al* 2015).

Silver sulfide nanoform has less reporting as bio-compatible material in *in*

vitro or *in vivo* applications. The hypothesized low toxicity with augmented potential of MS NPs, prompted us to plan the exploration of the silver sulfide nanoparticles and their composite with bioactive polymer against various phytopathogenic fungi relative to silver nanoparticles. The main objectives of the research work were:

1. To synthesize and characterize surface modified silver sulfide nanoparticles using different sources of sulphur
2. To evaluate antifungal potential of prepared silver sulfide nanoparticles against phytopathogenic fungi.

The thesis keeps running into few chapters, namely, review of literature, materials and methods, results and discussion and summary. Since, almost whole examination consolidated in the thesis is on the synthesis of silver sulfide and polymer coated silver sulfide nanoparticles and their antifungal activity, in this way the audit of writing was thought to be appropriate. The review of literature is specified as Chapter II. Chapter III comprises of methods of preparation of silver sulfide nanoparticles, various techniques used for characterization and antifungal activity of prepared samples. Results and discussion is given in the chapter IV. Chapter V summarizes the research work carried out. The references cited in the text are alphabetically arranged at the end of thesis.

CHAPTER-II

REVIEW OF LITERATURE

Ag_2S nanoparticles were obtained by an exchange reaction between sodium sulfide and silver nitrate. The prepared Ag_2S NPs were further coated with 3-mercaptopropyltrimethoxysilane. The main aim of this study was to determine the effect of hydrodynamic radii and zeta potential due to coating. The zeta potential of Ag_2S-MPS nanoparticles varied from -23.9 to +19.3 mV (Balyakin *et al* 2018).

Dehghanipour *et al* (2017) prepared Ag_2S nanoparticles using silver nitrate as precursor of silver ions and sodium thiosulfate as source of sulfur under strong stirring with TGA as capping agent. The prepared solution was irradiated with microwave radiation for 12 minutes and then centrifuged. The XRD pattern of Ag_2S showed monoclinic crystalline structure and exhibited absorption peak at 810 nm in UV-vis spectra.

One pot method was employed for the preparation of ultrathin Ag_2S nanoplatelets using 3-mercaptopropionic acid. XRD analysis depicted the β structure of Ag_2S nanoplatelets and the estimated thickness of nanoplatelets was 3.5 ± 0.2 (Kubie *et al* 2017).

One-pot route was employed for the synthesis of silver sulfide nanoparticles using (3-mercaptopropyl)trimethoxysilane (MPS) as capping agent, at pH = 4. Silver nitrate and sodium sulfide were used as the precursors for silver ions and sulfide ions respectively. The TEM images of MPS-capped Ag_2S nanoparticles synthesized showed spherical shaped nanoparticles with particle diameter from 2 to 10 nm. According to UV spectrum the absorption peak was observed in the range of 230-1250 nm (Kuznetsova *et al* 2017).

Xaba *et al* (2017) prepared silver sulfide-chitosan nanocomposite through modified homogeneous precipitation route to give spherical shaped with average size of 9.6 nm. Nanocomposites exhibited absorption band at 298 nm which was blue shifted from bulk with the value of 620 nm.

Jin *et al* (2016) reported the synthesis of Ag_2S quantum dots using thiourea by a facile aqueous synthesis method. The surface modification of Ag_2S QDs was done with polyethylenimine, followed by combination with the aptamer/5-Fu complex. TEM images exhibited spherical shaped monodisperse nanoparticles with average diameter of 5.5 nm. The XRD diffraction peaks revealed α-monoclinic structure. The EDX analysis of products showed the existence of Ag and S elements, and the Ag/S atomic ratio is close to the appropriate stoichiometry of Ag_2S bulk.

Karimipour *et al* (2016) carried out the synthesis of Ag_2S/ZnS core-shells by

facile microwave irradiation technique using thioglycolic acid (TGA) as capping agent. A strong absorption band was observed at 805 nm and emission located at 860 nm with a narrow width of 60 nm. XRD diffraction pattern showed the value of 2θ at 27.08° with monoclinic structure. The average size of synthesized core shells was in between 15-50 nm.

Silver sulfide nanoparticles were synthesized by the chemical reaction of AgNO3 (Ag+ ions) and $SC(NH_2)_2$ solution (S_2^- ions).The prepared Ag_2S nanoparticles were coated on TiO_2 spheres to enhance the photocatalytic activity. The crystal morphology of n-Ag2S/TiO2 composites was characterized by TEM, SEM, UV-VIS, XRD and XPS (X-ray photoelectron spectroscopy). HRTEM image clearly indicated the presence of highly crystalline structure with existence of good interface between TiO2 and Ag2S. XRD pattern revealed monoclinic structure of Ag_2S/TiO_2 composite (Ong *et al* 2016).

Sadovnikov *et al* (2016) synthesized non toxic silver sulfide nanoparticles by chemical condensation of aqueous solution of silver nitrate ($AgNO_3$) and sodium sulfide Na_2S in the presence of sodium citrate. The size of resulting nanoparticles was found to vary from 60 nm to 500 nm whose absorption peak varied from 360 nm to 460 nm.

Sadovnikov *et al* (2016) prepared the various forms of Ag_2S nanoparticles using hyydrochemical bath deposition method. Silver nitrate and sodium sulfide were used as Ag^+ and S^{2-} source respectively in aqueous form. Sodium Citrate was used as an electrostatic stabilizer and complexing agent. The particle size of nanoparticles varied from 200-1000 nm depending upon the concentration of Na_2S used. The formation of Ag_2S nanoform was proceeding through a simple reaction:

$$2AgNO_3 + Na_2S \longrightarrow Ag_2S\downarrow + 2NaNO_3$$

The another chemical route employed for the synthesis of silver sulfide nanoparticles involved the two step reaction methodology involving the synthesis of silver nanoparticles by dissolving solution of anhydrous silver nitrate in oleylamine solution, which was injected to sulfur solution of oleylamine at 100℃. The black colored reaction mixture, so obtained was stirred for 5 hours, cooled to room temperature and on addition of excess of methanol, black precipitates of the required product was obtained (Jang *et al* 2007) whereas the mixing of arsenic sulfide (As_2S_3) and silver chloride (AgCl) in propylamine was reported as single step method to produce highly crystalline silver sulfide (Ag_2S) nanoparticles (Almieda *et al* 2015).

Cui *et al* (2015) reported synthesis of Ag_2S nanostructures. The SEM images showed that the size of the nanoparticles ranged from 40 to 80 nm. The typical TEM images showed that most of the Ag_2S nanocrystals particles appeared hexagonal in

shape confirming the faceted nature of the nanocrystal. The UV–Vis absorption spectrum of the products showed obvious blue shift towards small size.

Sonochemical synthesis of the silver sulfide nanoparticles with the use of silver nitrate and thioacetic acid was reported by Emadi*et al* (2011) and Kristl *et al* (2015) presented the range of silver chalcogenides by using silver acetate and elemental chalcogens as precursors and ethylenediamine as solvent. The purity of the products was confirmed by energy-dispersive X-ray spectroscopy (EDX), X-ray powder diffraction (XRD) and atomic absorption spectroscopy (AAS) while the morphology of the products was studied by transmission electron microscopy (TEM). Monodisperse Ag_2Se nanoparticles and agglomerated Ag_2S and AgTe clusters were obtained in good yield.

Cu doped silver sulfide nanoparticles were synthesized via chemical coprecipitation method. The prepared sample was characterized by SEM, TEM, XRD, UV–vis spectra and EDX. From TEM images, the spherical shaped Ag_2S nanoparticles with an average diameter of 30 nm were observed. It was also demonstrated that the Cu doped Ag_2S nanoparticles had more antibacterial activity than un-doped Ag_2S nanoparticles (Fakhri *et al* 2015).

Murugadoss *et al* (2015) prepared novel ZnS/Ag_2S and Ag_2S/ZnS nanocoposites by using chemical method in air to nano forms of different morphologies of excellent photocatalytic and degradation properties. Krylova and Dukstiene (2012) deposited the Ag_2S on polypropylene surface by chemical bath deposition method to get analogue of Ag^+ ion selective electrode to be used in argentometric titration of thiamine hydrochloride.

Wang *et al* (2015) synthesized silver sulfide nanoparticles by the reaction of elemental sulfur with silver nitrate using polyvinylpyrrolidone as stabilizer and reported the size of nanoparticles from 60 to 100 nm.

Yadav *et al* (2015) carried out the synthesis of Ag_2S-TiO_2 nanocomposites by thermal decomposition method. The final product was characterized by transmission electron microscopy (TEM), diffuse reflectance spectroscopy (DRS), field emission scanning electron microscopy (FE-SEM), energy dispersive X-ray analysis (EDXA) and X-ray diffraction (XRD). Nanocrystalline structures of Ag_2S and TiO_2 was shown by XRD patterns. The particle size of Ag_2S nanoparticles in the TiO_2 matrix was 8.8 ± 1.9 nm. As compared to bulk Ag_2S, a blue shift of band gap was observed in the final nanocomposites.

A nanosecond (ns) pulsed laser ablation method was used for the synthesis of Ag_2S NPs dispersed in DMSO. The Z-scan method was applied to measure the non linear and linear optical coefficients, regime at 532 nm. The morphology of

nanoparticles was spherical in nature with an average size of 5.4 nm. The non linear optical properties of Ag_2S NPs make it deal in device fabrication and photonics (Aleali *et al* 2014).

Kumari *et al* (2014) synthesized silver sulfide nanoparticles by chemical co-precipitation method using sodium sulfide, silver nitrate and polyvinylpyrrolidone as stabilizer. All the nanoparticles were spherical in shape with average diameter of 30 nm and a broad peak between 450 nm to 500 nm.

Lv *et al* (2014) carried out the reaction of sodium sulfide nonahydrate and silver ammonia complex to get Ag_2S in nanoform. The reaction was done via hydrothermal method to get rice like morphology of Ag_2S. FT-IR, UV-Vis, TEM, EDX and XRD were used to characterized the prepared sample. From the TEM image, the average width of nanocrystals was 30-35 nm and length was 70-90 nm. FT-IR spectra showed various absorption peaks around 2972-2925 cm^{-1}, 1662 cm^{-1} and 1290 $cm^{-1.}$ XRD patterns revealed the formation of monoclinic α-Ag_2S.

A solvothermal method was used for the preparation of Ag_2S nanoparticles. Silver nitrate ($AgNO_3$) and a thio shiff-base named 2-benzylidene amino were used as initial components. The reaction was either proceeds in the presence of surfactant (CTAB or Polyethylene glycol) or in the absence of surfactant. The size of the nanoparticles was affected by the type of solvent used, presence of surfactant and react ion temperature (Shakouri-Arani and Salavati-Niasari, 2014).

Shebanova *et al* (2014) observed that the biosynthesized silver sulfide nanoparticles occurs in both aerobic and anaerobic conditions, using milli molar concentrated solutions of silver nitrate and sodium thiosulfate. It occurred significantly by *Shewanella oneidensis* MR-1 and the shape of the synthesized nanoparticles was spherical, having size 7.8±1.5 nm in the presence of living cells and it was 6.5±2 nm in the presence of ultrasonically disrupted cells.

Tan *et al* (2014) employed a cation-exchange method for the fabrication of silver sulfide nanowires. This cation exchange process involved a two-step reaction which gave the transformation of twinning nanowires. Cadmium sulfide nanowires were used as template to form Cu_2S-CdS core shell nanowires and consequently twinning Copper sulfide nanowires via cation exchange. The twinning Cu_2S nanowires were converted to Ag_2S-Cu_2S nanowires with tunable lengths via cation exchange of Ag^+ by Cu^+.

Liu *et al* (2013) reported the synthesis of Titanium dioxide nanotube arrays (TNAs) sensitized with Ag_2S nanoparticles using electrodeposition process and facile in situ sulfurization. TEM characterization of the final product revealed the nanoscopic arrangement of Ag_2S NPs on TNAs. Spherical shaped Ag_2S NPs with

uniform size of 5 nm were distributed homogeneously on both inside and outside of the nanotubes. The significance of loading on Ag_2S NPs on TNAs was that it enhanced the response of the TNAs to irradiation in the visible region and also improves the, photoelectrochemical, photovoltaic and photocatalysis applications.

Ng *et al* (2013) synthesized silver sulfide nanoparticles by using silver nitrate, sodium thiosulfate and *S. oneidensis* MR-1 as a model system. The nanoparticles showed a characteristic surface plasmon resonance band at 410 nm.

Verma *et al* (2013) reported chemical route for the synthesis of semiconducting silver sulfide nanoparticles and dispersion of silver sulfide nanoparticles in polyvinyl alcohol gave nanofluids. The average size of nanoparticles from TEM images was equal to 25 nm which corresponded to absorption band at 512 nm.

Self-assembled Ag_2S nanorods were successfully prepared using silver nitrate ($AgNO_3$) as source of silver and sodium sulfide as source of sulfide along with squalene by microwave assisted method. The synthesized α- Ag_2S nanorods were investigated by XRD, X-ray photoelectron spectroscopy (XPS), energy dispersion spectroscopy (EDS), electron diffraction (SAED), TEM and SEM. According to TEM measurements, Ag_2S nanorods had mean length of 31±2 nm and the average diameter was 10±1 nm. The stiochiometric composition of Ag_2S was 2:1, confirmed by XPS (Yaghmour *et al* 2013).

Yang *et al* (2013) synthesized Ag_2S nanoparticles using silver nitrate and thiourea via one-step hydrothermal synthesis. At different concentrations of surfactants various particle size of Ag_2S NPs were observed. TEM images showed the irregular spherical chain of Ag_2S NPs with average diameter in the range of 4-5 µm without any surfactant and in the presence of surfactant, the diameters decreased to the range of 1–3 µm.

Chaudhuri *et al* (2012) reported a novel method for the preparation of hollow Ag_2S nanoparticles via sacrificial core method with surfactant in aqueous media. A sacrificial core of sulfur nanoparticles was synthesized using $Na_2S_2O_3$ in CTAB and

$$Na_2S_2O_3 + 2HNO_3 \longrightarrow 2NaNO_3 + H_2SO_3 + S\downarrow \text{ (core)}$$

$$AgNO_3 + CTAB + Br^- \longrightarrow CTA^+ + AgBr\downarrow \text{ (shell)}$$

$$Ag(S_2O_3)^-, Ag(S_2O_3)^{3-} \longrightarrow Ag_2S + H_2SO_3 + H_2O$$

$$2AgBr + CS_2 \longrightarrow Ag_2S + CS + Br_2$$

after the formation of this core $AgNO_3$ was added. In order to get complete conversion of Ag_2S from AgBr, the above prepared mixture was treated with water ethanol mixture and carbon bisulfide (CS_2).

Ezenwa *et* al (2012) gave the synthesis of Ag_2S thin films deposited on glass substrates. This glass substrate was submerged in an aqueous bath mixture containing solutions of disodium salts of Ethylenediaminetetra-acetate, ammonia solution, Thiourea and silver nitrate. In this mixture, EDTA and ammonia were used as a chelating agent and pH adjustment respectively. The synthesized films showed absorption maxima at less than 400 nm and micrographs showed the grain size particles on the surface of sample. The mechanism for the synthesis of Ag_2S is as followed:

$$AgNO_3 + EDTA \rightleftharpoons Ag\,[EDTA]^{1+} + 3NO_3^-$$

$$Ag\,[EDTA]^{1+} \rightleftharpoons Ag^+ + EDTA$$

$$HS^- + OH^- \rightleftharpoons H_2O + S^{2-}$$

$$Ag^+ + S^{2-} \rightleftharpoons Ag_2S$$

Han *et al* (2012) carried out one-pot route for the preparation of core-shells of Ag_2S nanoparticles on nanospheres of mesoporous silica. Silver nitrate was used a source of silver ions, Na_2S as a sulfide ions source. In this synthesis, CTAB and formaldehyde were used as stabilizer and reducing agent respectively. The synthesized nanocrystals had monoclinic structure with average size of 17 nm.

In chemical process for the preparation of Ag_2S nanocrystals using silver thiobenzoate as precursor. The average particle diameters of the nanoparticles obtained were 9.2 ± 1.9, 8.3 ± 1.5 and 7.5 ± 0.9 nm depending on their reaction with octylamine, dioctylamine and oleylamine, respectively (Zhang *et al* 2012)

Size-controlled and monodispersed Ag_2S nanoparticles were synthesized via solventless thermolysis of various alkyl substituted silver xanthates. It was observed that Ag_2S nanoparticles prepared from silver octyl xanthate and silver hexa decyl xanthate have mean diameter of 48.3±3.6 nm and 19.5±0.9 nm respectively, whereas for the same product obtained from silver carnaubylase xanthate the mean diameter was 8.87±1.2nm. This indicated that the diameter of Ag_2S decreases with increase in the length of alkyl chain (Zhang *et al* 2012).

Ag_2S nanocrystals with worm like appearance were successfully synthesized by preparing a reverse microemulsion using cyclohexane/water/hexanol/Triton X-100 in the presence of thioacetamide and EDTA. The characterization of the prepared sample was done using TEM, UV-Vis and XRD. The size and shape of Ag_2S

nanocrystals were controlled by the molar ratio of surfactant, Ag^+: EDTA and aging time. The average diameter of Ag_2S nanofibres was 25-50 nm (Liu *et al* 2011).

Ag_2S nanowires were synthesized in anhydrous ethanol via sacrificial templating solvothermal method. The results of the experiment demonstrated that the Ag+ concentration, reaction temperature, solvent and reaction time played a vital role in the preparation of Ag_2S nanowires. In this process, a mixture of $Cd(CH_3COO)_2$ and S powder were dissolved in ethylenediamine. The obtained mixture was heated in autoclave for 2 h at 473 K. In the next step, the prepared $AgNO_3$ and CdS nanowires were dissolved in ethanol and then gain heated in autoclave for 2 h at 473 K. The CdS nanowires were completely transformed to Ag_2S nanowires after the addition of excess silver ions (Yan *et al* 2011).

Hashmi *et al* (2010) synthesized silver sulfide nanoparticles by colloidal synthesis technique at relatively low temperature by using chitosan bio polymer as stabilizer and the relative growth rates were controlled by suitable variation of chitosan concentration. All the nanoparticles were spherical in shape with size 2.5 micrometer to 300 nm.

Kim *et al* (2010) reported the presence of silver sulfide nanoparticles in wastewater treatment materials. The observed nanocrystals were characterized by TEM and EDX. The ellipsoidal shape of Ag_2S nanoparticles with size between 5-20 nm was confirmed by TEM analysis. From EDX analysis, the observed ratio of silver and sulfide was 2.1:1.7, which indicated the presence of excess Sulfur on the surface.

Leon-Velazquez *et al* (2010) studied the growth of silver sulfide nanoparticles by real time UV-Visible absorption measurements of stopped flows of silver nitrate and ammonium sulfide. The observed nanoparticles were in the range of 2 to 10 nm with the absorption band from 565 nm to 630 nm.

Sun *et al* (2010) prepared hollow Ag_2S nanohexagons in aqueous medium using CTAB. $AgNO_3$ was used as a precursor for Ag^+ and $Na_2S_2O_3$ as S^{2-} precursor. The product obtained was further characterized using TEM, FE-SEM and XRD. SEM analysis confirmed the presence of uniform hexagonal nanoparticles having edge to edge spacing of 48.9±1.82 nm and thickness equal to 36 nm.. The typical XRD patterns of Ag_2S nanohexagons were indexed to monoclinic phase.

A simple solution-phase method was employed for the formation of rhombic Ag_2S nanoparticles at 45 ◦C. The synthesized product was determined by TEM, FE-SEM and XRD. Rhombic morphology with uniform size distribution having edge length equals to 42.1±2.19 nm. TEM analysis revealed that these rhombus shaped nanoparticles were rounded corner and were hollow from inside. Concentration of CTAB in the reaction, decided the morphology of synthesized nanoparticles. Without

CTAB, small nanoparticles with disordered aggregation were observed and when 80-30 mM of CTAB was taken, rhombus shaped nanoparticles changed to worm like nanostructures (Sun *et al* 2010).

Yeo *et al* (2010) carried out the synthesis of aqueous Ag_2S nanoparticles using silver nitrate and thiourea. Various Ag_2S/PHB nanocomposites were also obtained through phase transfer of Ag_2S nanoparticles into PHB which contained diverse amounts of chloroform in it. Spherically and hexagonally shaped Ag_2S nanoparticles with particle size less than 24 were observed.

Anthony *et al* (2009) describes the nano array fabrication of 2-dimesional Ag_2S and Ag_2Se nanoparticles with self assembled block copolymer micelles. After the preparation of miceller solution and stirring at different temperatures, Silver nitrate was added to the micellar toluene solution and the filtered solution was layered on the Na_2S or NaHSe solution under inert atmosphere. The interactions between hydrophilic P4VP core with water were expected to expose the selenium ions and silver ions to sulfur and lead to the formation of Ag_2S or Ag_2Se nanoparticles. The obtained nanoparticles were in the crystalline form with dark brown color. The average diameter for the Ag_2S nanocystals were in the range of 2–4 nm and XRD patterns of Ag_2S showed the formation of monoclinic crystal structure of β-Ag_2S.

Kim *et al* (2009) synthesized Ag_2S, CuS, CdS and Cu_xS nanoparticles. The obtained nano suspensions of metal sulfides were stabilized by green synthesized dextran bioplolymer. The size of Ag_2S, CdS, Cu_2S nanoparticles were 20–50 , 9, 14 nm respectively , and the homogeneous morphology of CuS with average size of 9-27 nm was observed. FT-IR analysis predicted metal-sulfide bands over 500-600 cm^{-1} and with dextran, a strong band was observed at 1000–1100 cm^{-1}.

Chen *et al* (2008) described a fast, simple procedure for obtaining an assembly Ag_2SNPs on a glass substrate through reaction of a template of an assembled layer of silver nanoparticles (Ag NPs) with H_2S gas. The Ag NP template was prepared by assembling a monolayer of spherical Ag NPs (mean diameter of 7.4 nm) on a polyethylenimine-treated glass substrate. Exposure to pure H_2S for 10 min converted the Ag NPs of the template to Ag_2S NPs. The NPs have a crystal structure of monoclinic acanthite, and while they retained the spherical shape of the original Ag NPs, their mean particle size increased to 8.4 nm due to changes to the crystal structure when the Ag NPs are converted into Ag_2S NPs.

Dong *et al* (2008) gave the synthesis of Ag_2S nanoparticles using thiourea as sulfide ion source and $AgNO_3$ as silver source via hydrothermal route. The TEM images showed the formation of nanocubes and faceted nanocrystals with absorption peaks at 375 and 325 nm respectively in the UV-Vis spectra. SEM analysis predicted

that the particle size of Ag_2S nanoparticles was about 40 to 80 nm and its molar ratio was 67.49 to 32.51.

Ag_2S nanoparticles were obtained by heating silver diethyldithiocarbamate for 3 hours in air at 473 K and the air stabilized precursor was used as a reactant. The obtained nanocrystals were characterized by Fourier transform infrared spectroscopy (FTIR), powder X-ray diffraction (XRD), thermo gravimetric and differential scanning calorimetry (TG-DSC) and field emission scanning electron microscope (FESEM). FESEM image indicated the presence of crystalline α-Ag_2S powders with average size in between 20 nm to 1.1μm. From TG–DSC data, a curve in between 30–1000 °C confirmed the presence of α- Ag_2S powders with negligible weight loss and in DSC curve a peak at 181 °C was due to phase transition from α to β form of Ag_2S (Wang *et al* 2008).

Wang *et al* (2008) reported the synthesis NiS_2/Ag_2S composites using Ag_2S nanospheres and hollow nickel disulfide microspheres as precursors. The microstructures and morphologies of Ag_2S nanospheres and NiS_2 microspheres were demonstrated by TEM and SEM images. From SEM image, the average size of Ag_2S nanospheres was 100 nm.

Wang *et al* (2008) used warm octadecylamine to dissolve $AgNO_3$ to form silver ammines that were rapidly transformed to Ag_2S nuclei after the addition of Sulfur powder. The reaction mixture should keep at 393 K for the further crystallization and growth. After the completion of the reaction, ultralong Ag_2S nanowires were obtained. The average diameters were in the range of 10–30 nm. The main disadvantage of this process was that these nanowires could only be obtained at 393 K. These nanowires exhibited an excellent performance in the field of photoswitches.

Xiaodong *et al* (2008) reported the synthesis of well-dispersed aqueous Ag_2S nanocrystals using thioacetamide as sulfide ion source, silver nitrate as silver ion source and imidazoline as surfactant. The product obtained was characterized by FT-IR, TEM and XRD. From TEM image it was observed that without surfactant Ag_2S nanocrystals were in aggregate form with irregular shape and on increasing the concentration of surfactant, the size gradually decreases because of the separation of aggregate molecules. XRD patterns indexed to the monoclinic structure and broad peaks indicated the small nano size of Ag_2S crystals. In UV-Vis spectra an absorption peak at 260 nm was also observed.

Zhai *et al* (2007) carried the synthesis of nano and micro Ag_2S materials via facile one-step method. To characterize the composition and structures of the synthesized products, various analysis like SEM, XPS and XRD were employed.

Different morphologies like nanowires, nanopolyhedrons, worm-like nanoparticles, micrometer bars, and microfibers of Ag_2S materials had been observed and they showed diverse spectral features in UV-Vis spectra. XPS further favoured the formation of Ag_2S nanoparticles by exhibiting the ratio of integral area of Ag:S equals to 2:1. Broad peaks in XRD patterns revealed the presence of nanosized materials.

Zhao *et al* (2007) reported the chemical reaction of S^{2-} generated from dispersed $S_2O_3^{2-}$ ions with Ag+ to give Ag_2S nanoparticles. Ag_2S nanorods showed blue shift towards 490–520 nm in UV–Vis absorption spectrum. From TEM images, non uniform nanorods with diameter 200 to 500 nm were observed and SAED patterns indicated the formation of polycrystalline Ag_2S nanorods. In XRD patterns, all the peaks with lattice constants of 0.68 nm, 0.77 nm and 0.41 nm indexed to the monoclinic Ag_2S nanoparticles.

Zhao *et al* (2007) gave the synthesis of Ag_2S nanocrystallines with rod like morphology via gamma ray irradiation using aqueous solution of $Na_2S_2O_3$ as sulfide ion precursor. The monoclinic Ag_2S structure was confirmed by the lattice constants obtained from XRD analysis. The resulting nanorods were non-uniform in nature with diameter ranged from 200 to 500 nm. The UV-vis analysis showed an obvious blue shift in the spectrum.

Zhaung *et al* (2007) employed the synthesis of tetrahedral colloidal Ag_2S nanocrystals using silver nitrate, 1-dodecanethiol and ammonia at 473 K in an autoclave. DLS analysis indicated the formation of aggregated Ag_2S nanoparticles in triangular morphology with edge length in between 100-1000 nm. The average diameter of 3.5±0.5 was shown by TEM studies.

Synthesis and conjugation of silver sulfide nanorods with protein named Bovine Serum Albumin (BSA) was observed. The whole procedure involved a two step reaction. In first step, there was the formation of Ag(I)-BSA complex and then in second step, thioacetamide was added as S^{2-} ion source. Nanosized rod like structure of Ag_2S was confirmed by SEM analysis. TEM analysis predicted monodispersed Ag_2S nanorods with average diameter and length of 40 and 220 nm respectively. According to UV spectroscopy, a sharp emission peak was observed at 474 nm (Yang *et al* 2006).

Chen *et al* (2006) carried out the synthesis of leaf shaped Ag_2S nanosheets. The whole reaction was carried out via hydrothermal route in water-alcohol medium. In this synthesis, CS_2 was used as a sulfur ion source and $AgNO_3$ as silver ion precursor. The UV–vis spectrum showed an absorption peak at 275 nm and from XPS analysis, the ratio of 1.8:1 confirmed the formation of Ag_2S.

$$2NH_3 + CS_2 \longrightarrow NH_4NHCSSH$$

$$2AgNO_3 + NH_4NHCSSH \longrightarrow Ag_2S + NH_4SCN + NH^{4+}$$

Ding *et al* (2005) synthesized Ag_2S nanoparticles using $AgNO_3$ and Na_2S in lamellar liquid crystals. The TEM images showed that the prepared nanoparticles were spherical in shape with an average size of 2-3 nm. Further XRD analysis confirmed the crystalline structure of Ag_2S nanoparticles.

Tang *et al* (2005) reported the synthesis of Ag and Ag_2S nanocrystals using silver monothiobenzoate (Ag(SCOPh)) as single molecular precursor via modified hot-injection process . In contrast to Ag nanocrystals which showed low homogeneity in shape, Ag_2S nanocrystals revealed much uniformity in shape. The average diameter of Ag_2S nanocrystals was 25 nm whereas for that of Ag nanoparticles it was about 80 nm.

Monodispersed Ag_2S nanoparticles were successfully synthesized by thermolysis of single precursor i.e. silver(I) dialkyldithiophosphate. These grain sized Ag_2S nanoparticles had an average diameter of 14.3 ± 0.7 nm (Wang *et al* 2005).

Wang *et al* (2005) employed an improved hydrothermal method for the preparation of nanostructured Ag_2S. Silver sulfide nanocrystals with size 7.3 nm were synthesized by the use of a liquid–solid–solution system, which contained solid metal linoleate, water–ethanol solution and ethanol–linoleic phase. The synthesized nanoparticles were monodispersed and uniformly distributed.

Wen *et al* (2005) reported a successful method synthesis of Ag_2S in the form of nanowires using gas–solid reaction process on silver substrates. For the synthesis of nanowires, a cleaned silver foil was firstly subjected to sulfidizing and preoxidation by an exposure in the atmosphere of O_2/H_2S mixture in water bath kept at 313 K. The diameter and length of resulting Ag_2S nanowires was 40-150 nm and 100 nm respectively. XRD analysis revealed that Ag_2S nanowires had monoclinic acanthite structure.

Fang *et al* (2004) developed a minigel template method for the synthesis of Ag_2S–poly(N-isopropylacrylamide-co-methacrylic acid) and Ag_2S–poly(N-isopropylacrylamide) composites. The surface morphology of these microspheres was not depending only on the nature of template but it was also affected by the nature of metal sulfides. In this process minigels play a vital role for the precipitation of metal sulfides. The flower like morphology was appeared on the surface of these microspheres.

Lim *et al* (2004) observed that at room temperature silver thiobenzoate (Ag(SCCOPh)) readily decompose in amine to give Ag_2S nanoparticles. The main parameters of this reaction are the type of amine used, temperature during synthesis,

reaction time etc. TEM results showed the uniform synthesis of cubed-shaped Ag_2S nanoparticles with an average size of 44±4 nm. The reaction temperature played at important role in the synthesis of shape and size controlled silver sulfide nanoparticles. A monoclinic acanthite Ag_2S structure was observed from the X-ray analysis.

$$2\ Ag(SCOPh) + 2\ CH_3(CH_2)_{15}NH_2 \longrightarrow Ag_2S + 2\ CH_3(CH_2)_{15}NHCOPh + H_2S$$

A simple aqueous precipitation method was adopted for synthesizing a series of silver sulfide nanoparticles with varied sizes. Silver nitrate was used a precursor of silver ions and ammonium sulfide as a precursor of sulfide ions, followed by stabilization. Three different stabilizing agents i.e. Triton X-100, 3-mercapto-1, 2-propanediol and mercaptoacetic acid were used for controlling particle size. The synthesized particles were characterized by SEM, XRD, TEM. XRD analysis predicted the monoclinic structure of nanoparticles, which was the stable form of silver sulfide. The TEM images showed spherical and ellipsoidal shaped nanoparticles with size range between 20-50 nm (Martınez-Castanon *et al* 2004).

Aqueous Ag_2S nanocubes were synthesized by the chemical reaction of silver nitrate and thioacetamide in the presence of carboxymethyl cellolose as capping agent. TEM images showed a large number of cubic hollow shaped structures with the edge length of approximately 200±50 nm. From SEM photograph, a “frame” like arrangement, which was hollow from inside and had holes on each edge was observed. The effect of temperature on Ag_2S nanocubes was also studied. When the synthesis was carried out at low temperature, concave microstructure was obtained and when the reaction was carried out at 80ºC (or higher), hollow Ag_2S nanocubes were obtained. In UV-Vis spectra, absorption peaks for both samples were observed at 260 and 285 nm, respectively (Wu *et al* 2004).

Xu *et al* (2004) also reported alcohol solution method for the preparation of Ag_2S using CS_2 as sulfur source, with all the products having irregular shapes. The reaction medium was changed from water and alcohol–water to alcohol. So, the morphology changed from big irregular nanosheets and microspheres, leaf-like nanosheets nanoparticles to big microspheres, respectively. It is found that alcohol–water homogenous condition and sulfur source of NH_3-CS_2 played the key roles in constructing this unique morphology. That is because the formation of nucleation and growth is expected to be strongly dependent on the properties of the solvent during processes such as coarsening and aggregation (Cheng *et al* 2004, Wong *et al* 1998).

Schaaff and Rodinone (2003) synthesized the silver sulfide nanocrystals using silver thiolate polymers with sodium sulfide in a dual-phase solution preparation. From transmission electron microscopy and laser desorption ionization mass

spectrometry, the mean nanocrystalline diameter was estimated to be 5.4 nm.

The hydrogen sulfide (H_2S) gas diffusion method was employed for the synthesis of silver sulfide (Ag_2S) nanoparticles dispersed in sol-gel derived hydroxypropyl cellulose (HPC)-silica films with silver nitrate ($AgNO_3$) precursor. Transmission electron microscope (TEM) and atomic force microscope (AFM) analysis revealed nanoparticles size distribution from 2.5 nm to 56 nm (Shukla *et al* 2002).

Zhang *et al* (2000) successfully synthesized Ag_2S nanocrystals via quick precipitation reaction of aqueous silver complex solution and alkaline sulfur solution. The product was characterized through TEM, XPS and XRD analysis. TEM image showed agglomerated crystals with particle size of 80 nm. From XRD patterns, values of lattice constants and the broadening of diffraction peaks clearly indicated the presence nanosized particles. XPS analysis exhibited strong peaks at 160.7 eV and 367.8 eV, which corresponds to the formation of Ag_2S nanocrystals.

Akamatsu *et al* (1999) reported nylon dispersed silver sulfide nanoparticles. Electron diffraction patterns depicted β-Ag_2S nanoparticles with monoclinic structure and according to quantitative EDX analysis; the ratio of silver to sulfur was 2:1, which further confirmed the exact stoichiometric ratio of silver sulfide. The average diameter of silver sulfide nanoparticles was 4.7±11.2 nm.

Brelle *et al* (1999) carried out a synthetic method for the preparation of Ag_2S nanoparticles capped with glutathione or cystein via two steps synthesis. In the first step, there was stoichiometrically formation of metal-thiolate using thiol as sulfide source and silver acetate as a source of silver ions and in the second step the prepared mixture in the first step was titrated with Tris buffer. The particle size was about 9 nm and the electron diffraction patterns revealed the crystalline structure of Ag_2S nanoparticles.

Pileni *et al* (1996) reported the synthesis of silver sulfide nanoparticles using reverse micelles. Fluorescence spectroscopy and TEM micrographs were used to evaluate the formation of silver sulfide nanoparticles. The 2D and 3D self-assemblies composed of silver sulfide nanoparticles coated with dodecanethiol were observed. From Fluorescence spectroscopy, it was found that 2D monolayers were organized in a hexagonal network and 3D layers formed a face-centered cubic structure. The average particle size observed from TEM images was 2.3 nm and the interparticle size was 2 nm.

Biological synthesis of silver sulfide nanoparticles

Debabov *et al* (2013) employed the metal-reducing bacterium Shewanella *oneidensis* MR-1 to obtain Ag_2S nanoparticles from an aqueous solution of $AgNO_3$

and $Na_2S_2O_3$ at an ordinary temperature and pressure. The nanoparticles vary in size within 2–16 nm, and the fraction 6 to 12 nm in size constitutes about 70%. The particles obtained were like spheres with average diameters varying from 7 ± 2 nm to 9 ± 2 nm. Changes in the reaction conditions (reagent concentrations, temperature, and cell-incubation time in the reaction mixture) influence the yield of nanoparticles dramatically, but have little influence on their size. Following the similar methodology Suresh *et al* (2011) synthesized silver sulfide nanoparticles by using silver nitrate, sodium thiosulfate and metal reducing bacterium *Shewanel laoneidensis* culture. The average diameter of synthesized spherical shaped nanoparticles capped by peptide surface coat was 9±3.5 nm.

The green methods used for the synthesis of Ag_2S nanoparticles involved the pomosynthetic procedure, using Passiflora tripartitavar. mollissima fruit pigments as both the reducing and stabilizing agents (Kumar *et al* 2015) whereas *Shewanella oneidensis* MR-1 has been employed to obtain Ag_2S nanoparticles from an aqueous solution of $AgNO_3$ and $Na_2S_2O_3$ at ordinary pressure and temperature. The nanoparticles vary in size between 2–16 nm and about 70% of the particles were in the range of 6 to 12 nm. For the formation of Ag_2S nanoparticles the presence of living bacterial cells was obligatory in aqueous salt solution.

A green synthesis for size-controlled and monodispersed Ag_2S nanoparticles was done successfully using a single source precursor (silver xanthates) via surfactant and solvent free thermolysis. In the experiment, Ag_2S nanoparticles were characterized using TEM, FTIR and XRD. The size of Ag_2S nanoparticles was controlled by the alkyl chain length of reactants. Ag_2S nanoparticles prepared from silver octyl xanthate and silver hexadecyl xanthate exhibited a mean diameter of 48.373 nm and 19.570 nm respectively, whereas, in case of silver carnaubyl xanthate the mean diameter was 8.971.2 nm (Zhang *et al* 2012).

Biological activity of silver sulfide nanoparticles

Xaba *et al* (2017) examined that the improvement in antimicrobial effect can be achieved when a polymer was formed by the the incorporation of silver sulfide nanoparticles with chitosan. Fe^{2+} were removed from water and the results showed that in comparison to purer chitosan, silver sulfide-chitosan nanocomposites were better biosorbent.

Sadovnikov *et al* (2016) examined that the citrate capped 0.1 millimol/litre silver sulfide nanoparticles showed antibacterial activity against *E. coli* (Gram-negative bacteria).

Kumar *et al* (2015) evaluated the antioxidant activity of Ag_2S against 1,1-diphenyl-2- picrylhydrazyl (DPPH). Maximum percentage of free radical scavenging

activity was 66.93 % for 0.15 mM AgNPs. The antioxidant activity against DPPH is probably derived, through the electrostatic attraction between neutral or positively charged nanoparticles and negatively charged bioactive compounds (COO^-, O^-).

Wang *et al* (2015) studied that the direct accumulation of silver sulfide nanoparticles in terrestrial plant tissues exerts toxic effects. This study demonstrated that silver sulfide nanoparticles pose a risk through food chain as well as to plants.

Kumari *et al* (2014) examined that the growth inhibition of more than 75% against *E. coli* (ATCC 13534), *E. coli* (ATCC 25922) and *S. aureus* (ATCC 25923) was shown by 0.1 microgram/ml of the silver sulfide nanoparticles.

Suresh *et al* (2011) examined that silver sulfide nanoparticles did not show any significant activity against *S. oneidensis*, *E. coli* and *B. subtilis*. The main advantage of silver sulfide nanoparticles was that they can be used in various bio-labeling and bio-imaging.

Synthesis of silver nanoparticles

Hebeish *et al* (2016) established a technique devoted to one-pot green synthesis of dry highly stable powdered silver nanoparticles, using starch as reducing and stabilizing agent in the presence of NaOH. The alkali treated starch added to $AgNO_3$ solution, which induced well-established dual role; reduction of silver ions (Ag^+) to AgNPs and capping the as-formed AgNPs to prevent them from further growth and agglomeration.

A one-step route for the green synthesis of nanosized and highly stable chondroitin sulfate capped silver nanoparticles with narrow distribution is reported by Cheng *et al* (2014). Biocompatible chondroitin sulfate was used as both reducing agent and stabilizing agent to form spherical shaped AgNPs of an average size less than 20 nm.

Farasat and Golzan (2014) reported a new, direct, simple and high yield solution phase synthesis for preparing narrow-sized methyltrimethoxysilane capped silver nanoparticles by reduction with aqueous solution of $AgNO_3$ in the presence methyltrimethoxysilane (MTMS) at room temperature. The resulted MTMS-silver nanoparticles were well dispersed with an average diameter of 15 nm, and showed broad surface plasmon resonance bands in UV–visible spectrum.

Yan *et al* (2014) demonstrated the effect of reducing agents and surfactants on direction and growth rate of the silver nanoplates using trisodium citrate dehydrate and potassium tartrate as a reducing agent, and polyvinyl pyrrolidone and sodium dodecyl sulfate as surfactants.

Toh *et al* (2014) investigated the interactions between citrate capped silver nanoparticles and two different thiols, cysteine and mercaptohexanol (MH). The thiol

MH, formed a sparingly soluble silver(I) thiolate complex $AgSR_m$ ($R_m = -(CH_2)_6OH$) on the silver nanoparticles surface and cysteine replaced the citrate from the surface of silver nanoparticles, and resulted cysteine capped nanoparticles. The electrochemical data displayed a continuous decrease in oxidative peak charge but a constant signal in UV-Visible spectra indicated that cysteine inactivated the silver surface or promoted detachment from the electrode surface.

Aramwit *et al* (2014) synthesized the silk sericin-capped silver nanoparticles under an alkaline condition (pH 11) using silk sericin (SS) itself as a reducing and stabilizing agent. The SS-capped Ag NPs showed a spherical shape and having diameter around 48 to 117 nm.

Agasti *et al* (2014) synthesized the water soluble silver nanoparticles assisted by reduction of $AgNO_3$ with $NaBH_4$ in aqueous solution under atmospheric air in the presence of glycine.

Kora and Rastogi (2013) also synthesized silver nanoparticles by reducing $AgNO_3$ with $NaBH_4$ in the presence of capping agents such as citrate, sodium dodecyl sulfate (SDS) and polyvinylpyrrolidone (PVP). The produced nanoparticles were found to be spherical in shape and polydisperse with variable size.

Patil *et al* (2012) synthesized silver nanoparticles by using hydrazine hydrate as reducing agent and polyvinyl alcohol as stabilizing agent at room temperature. The synthesized silver nanoparticles had face-centered cubic (FCC) structure that showed surface plasmon resonance at 410nm. The diameter of spherical shaped AgNPs were in range of 10-60nm.

Malina *et al* (2012) synthesized silver nanoparticles and investigated from the position of surface plasmon resonance band that particle size depends upon PVP concentration and it has a significant influence on silver nanoparticles morphology and optical properties.

Chandra and Kumar (2011) reported green approach for synthesis of highly concentrated and stable suspension of AgNPs by chemical reduction of $AgNO_3$ in a reductant using a macrocyclic Schiff base ligand benzildiethylenetriamine and thiosalicylic acid as protective agent. The particles were found to have an average size of less than 20nm.

Kasture *et al* (2008) synthesized capped silver nanoparticles using sophorolipids (oleic acid and linoleic acid derived sophorolipid) as reducing and capping agents. The effect of structure of sophorolipid and the temperature on the size of silver nanoparticles was studied.

Bhata and Maitra (2008) synthesized amphiphilic thiol capped gold and silver nanoparticles, series of bile acid-derived facially amphiphilic thiols was used to cap

silver and gold nanoparticles. The self-assembling properties of these steroid-capped nanoparticles were investigated.

Li *et al* (2003) synthesized mercapto acetic acid-capped spherical silver nanoparticles with a diameter of about 17 nm and polyvinylpyrrolidone (PVP)-capped silver spherical nanoparticles and nanorods were synthesized that serve as active catalysts for polymerization of alkyl silane $C_{18}H_{37}SiH_3$ with water, to give flower petal-like composite siloxane microspheres.

Wang *et al* (1999) synthesized long chain unsaturated carboxylate capped silver nanoparticles in which the cis configuration of unsaturated carboxylates was found to be useful stabilizers for the control of particle size and its surface properties.

Biological activity of silver nanoparticles

Sundar *et al* (2016) synthesized 5-methyl 2-mercapto benzimidazole capped Silver nanoparticles via chemical reduction. Spherical shaped capped Ag NPs with size of 40 nm were obtained by treatment of aqueous silver ions with ethanolic solution of 5-methyl 2-mercapto benzimidazole as capping agent. The obtained silver nanoparticles were uniform in their sizes and shape and inflicted the antibacterial properties.

Sibiya *et al* (2016) reported green synthetic approach for starch capped silver nanoparticles. The Ag NPs showed surface plasmon resonance peak at 400nm. The Ag NPs also showed antibacterial activity against the tested Gram-negative and Gram positive bacteria.

Saha *et al* (2016) investigated that putrescine capped silver nanoparticles and found them to be more efficient and interactive antibacterial potentiality than bare ones.

Elgorbana *et al* (2016) tested silver nanoparticles at concentrations 0.0, 0.0002, 0.0005, 0.0007, 0.0009, 0.0014 and 0.0019 mol/L against six different *Rhizoctonia solani* anastomosis groups infecting cotton plants on czapek dox agar (CDA) and potato dextrose agar plates and showed strong inhibition of *R. solani* on CDA at all concentrations.

Mahdizadeh *et al* (2015) checked *in vitro* antifungal activity of silver nanoparticles, at concentrations 6, 8, 10, 12, 14 and 16 ppm for phytopathogenic fungi *viz.Macrophomina phaseolina*, *Sclerotinia sclerotiorume* and *Pythium aphanidermatu*. The fungal isolates were grown on potato dextrose agar medium amended with silver nanoparticles. Radial fungal growth was recorded after 1, 2, 3, 5 and 10 days and mycelial growth inhibition rates were calculated. The most sensitive fungus to nanoparticles was *P. aphanidermatu*, second most sensitive fungus was *S. sclerotiorume* and *M. phaseolina* was the third in sensitivity.

Polyvinyl pyrrolidone capped silver nanoparticles having average diameter 10 nm exhibited a tremendous potential antibacterial activity against the carbapenem resistant strain of *Acinetobacterbaumannii*, so can be used as an alternative to antibiotic carbapenem (Tiwari *et al* 2014).

Naz *et al* (2014) reported the synthesis of bioactive silver capped nanoconjugates with 5-Amino-β-resorcylic acid hydrochloride dehydrate (AR). Nanoconjugates showed significantly enhanced biological activity in comparison to free drug molecules. In *vitro* antimicrobial (antifungal, antibacterial), enzyme inhibition (α-chymotrypsin, urease, xanthine oxidase, carbonic anhydrase, cholinesterase) and antioxidant activities of the developed nanostructures were investigated before and after conjugation to silver metal.

Aashritha *et al* (2013) evaluated antifungal activity of silver nanoparticles synthesized by chemical reduction method, using silver nitrate and sodium citrate.

The polyethylene glycol (PEG) and TritonX-100 (TX) capped nanoparticles were synthesized via chemical reduction method using different concentrations (0.3, 0.6 and 0.9 mM) of polyethylene glycol (PEG) and TritonX-100 (TX). The antimicrobial activities of these capped silver nanoparticles homogenized with collagen were tested against both Gram positive and negative bacteria (Mandal *et al* 2013).

Das *et al* (2013) synthesized linoleic acid capped silver nanoparticles by chemical reduction of silver ions by ethanol using linoleic acid as a stabilising agent. Linoleic acid capped silver nanoparticles had high antimicrobial activity against *E. coli* and *S. aureus*.

Dextran-capped silver nanoparticles were synthesized by reducing silver nitrate with $NaBH_4$ using dextran as capping agent. The resulting nanoparticles showed uniform shape with narrow size distribution and better stability in comparison with polyvinylpyrrolidone (PVP) capped silver nanoparticles. The dextran-capped silver nanoparticles had high antibacterial activity against *Escherichia coli, Staphylococcus aureus, Staphylococcus epidermidis, Pseudomonas aeruginosa* and *Klebsiella pneumoniae* (Yang *et al* 2012).

Kim *et al* (2012) evaluated the antifungal efficacy of silver nanoparticles WA-AT-WB13R, WA-CV-WA13B and WA-PR-WB13R at concentrations of 10, 25, 50, and 100ppm against eighteen different plant pathogenic fungi on potato dextrose agar (PDA), malt extract agar, and corn meal agar plates and indicated that Ag NPs showed antifungal properties against these plant pathogens at all concentrations. Treatment with WA-CV-WB13R AgNPs resulted in maximum inhibition plant pathogenic fungi at 100 ppm.

Silver nanoparticles of various sizes were synthesized by using different molar concentrations of NaOH while changing the temperature. $AgNO_3$, gelatine, glucose and NaOH were used as a silver precursor, stabilizer, reducing agent and accelerator, respectively (Vasireddy *et al* 2012).

Dini *et al* (2011) reported the green chemistry approach to synthesize capped silver nanoparticles using saccharides as reducing and capping agent. Silver nanopparticles (AgNPs) cytotoxicity related to saccharides capping (Glucose (G) and Glucose-Sucrose(GS)) was explored in human epitheloid cervix carcinoma cells (HeLa) and the degree of the toxicity of AgNPs capped with Glucose were found to be more than that of Glucose-Sucrose capped nanoparticles.

Silver nanoparticles of an average size 12 nm have been prepared through the chemical reduction of Ag^+ ions by ethanol in presence of sodium linoleate. The antimicrobial activity of silver nanoparticles showed that these nanoparticles can be used as effective growth inhibitors against *Staphylococcus Bacillus*, *Staphylloccoccus aureus* and *Pseudomonas aureginosa* (Das *et al* 2011).

Nasrollahi *et al* (2011) investigated the antifungal effects of silver nanoparticles on *Candida albicans*(ATCC 5027) and *Saccharomyces cerevisiae* (ATCC 5027) by using minimum inhibitory concentration (MIC) technique and indicated that Ag-NPs showed better antifungal activity comparison with other antifungal drugs.

Mallmann *et al* (2010) reported new routes to synthesize silver nanoparticles, using nontoxic compounds ribose as a reducing agent and sodium dodecyl sulfate (SDS) as a stabilizing agent. The obtained stable nanoparticles 12.5 ± 4.9 nm (mean ± SD) in size were evaluated for antifungal activity against *Candida albicans* and *Candida tropicalis*. AgNPs showed high activity and represented an alternative for fungal infection treatment.

The cysteine capped silver nano-particles were synthesized by reduction of $AgNO_3$ using $NaBH_4$ as a reducing agent and cysteine as a capping agent (stabilizer). The so-prepared Cysteine bound silver nanoparticles (17ppm Ag in Cysteine) enhanced the anti mycobacterial activity of cysteine from 10 ppm to about 6 ppm (Varghese *et al* 2009).

Silver nanoparticles were prepared by chemical reduction method using silver nitrate as the metal precursor and hydrazine hydrate as a reducing agent. The UV-Vis spectroscopy revealed the formation of silver nanoparticles by exhibiting the typical surface plasmon absorption maxima at 418-420 nm. TEM images indicated that the diameter of silver nanoparticles in colloidal solution was about 60 nm. The silver nanoparticles showed high antimicrobial activity against gram positive bacteria such

as *Escherichia Coli*, *Pseudimonas aureginosa* and *Staphylococcus aureus* which is a highly methicillin resistant strain (Guzman *et al* 2009).

Biological activity of Chitosan

Azuma *et al* (2015) reviewed about the antitumor activity of COS *in vivo* and *in vitro* cell models showing effectiveness on tumor growing, reduction of the number of metastatic colonies, suppressing cancer cell growing, and enhancement of acquired immunity.

A novel theory was proposed about the inhibition mechanism of chitosan, that is, an inhibition of RNA and protein synthesis by permeation into the cell nucleus and eventually rupture and leakage of intracellular component. In this theory, the MW is the most decisive factor on the activity (Younes *et al* (2015), Aranaz *et al* (2010) and Aranaz *et al* (2009).

Younes *et al* (2014) and Jung *et al* (2010) also achieved similar results about the antimicrobial activity depending on chitosan DDA. When the DDA was nearly 100% (99%), chitosan inhibited almost all types of bacteria tested at the minimum inhibitory concentration (MIC).

Friedman *et al* (2013) reported the inhibition capacity of chitosan-alginate nanoparticles against inflammatory cytokines and chemokines induced by P. acnes, and the results showed that chitosan-alginate nanoparticles efficiently inhibited P. acnes-induced cytokine production in human monocytes and keratinocyte in a dose-dependent manner.

Benhabile *et al* (2012) experimented the antimicrobial potential of chitin, chitosan, and its N-acetyl chito- and chito-oligomers against four Gram-positive bacteria (Staphylococcus aureus ATCC 25923 and ATCC 43300, Bacillus subtilis, and Bacillus cereus) and seven Gram-negative bacteria (Escherichia coli, Pseudomonas aeruginosa, Salmonella typhimurium, Vibrio cholerae, Shigella dysenteriae, Prevotella melaninogenica, and Bacteroides fragilis).

Oliveira *et al* (2012) examined the inhibition of proinflammatory cytokines and anti-inflammatory activities of chitosan film. From the achieved results, a reduction of TNF-α (proinflammatory cytokines) in 3~10 days of cells cultured on chitosan film and significant increase of anti-inflammatory cytokines IL-10 and TGF-β1 are presented.

Park *et al* (2011) investigated the effects of the DDA and MW of chitosan oligomers on antitumor activity. The lower MW and higher DDA (higher solubility) were promising factors for the development of antitumor agents derived from chitosan in *in vitro* tests with Human PC3 (prostate cancer cell), A549 (carcinomic human alveolar basal epithelial cell), and HepG2 (hepatocellular carcinoma cell).

Xu *et al* (2010) described that the antitumor activity of chitosan nanoparticles might be related to antiangiogenic activity that is correlated with vascular endothelial growth factor receptor (VEGFR2) production and subsequent blockage of vascular endothelial growth factor- (VEGF-) induced endothelial cell activation.

Takahashi *et al* (2008) tested the influence of DDA of chitosan on the antimicrobial activity against *Staphylococcus aureus* using two different testing methods, that is, incubation using a mannitol salt agar medium and a conductometric assay. In both testing methods, the DDA of chitosan played a dominant role in the inhibition of *Staphylococcus aureus* growing (the higher DDA showed the higher rate of inhibition).

Liu *et al* (2006) studied that both N-acetyl chito and chito-oligomers were more effective on the inhibition activity against all tested microorganism than chitosan and chitin, and the decisive effect of DDA and MW on antimicrobial activity was well proved.

CHAPTER-III

MATERIALS AND METHODS

Chemicals and reagents

The chemicals and reagents used were of AR or LR grades. List of these chemicals and reagents is given below:

i. Silver nitrate- Loba Chemie Pvt. Ltd, Mumbai.
ii. Triton X 100 - Molychem, Mumbai.
iii. Sodium sulfide - Loba Chemie Pvt. Ltd, Mumbai
iv. Thiourea - Central Drug House Pvt. Ltd, New Delhi
v. Thioacetamide - Loba Chemie Pvt. Ltd, Mumbai
vi. Sodium thiosulfate - Thomas baker chemicals Ltd, Mumbai
vii. Polyvinyl pyrollidone - SISCO Research Laboratries Pvt. Ltd, Andheri
viii. Chitosan - Loba Chemie Pvt. Ltd, Mumbai

Characterization techniques

Various characterization techniques were employed for characterization of silver sulfide nanoparticles (Ag_2S NPs), which are discussed below:

i. Transmission Electron Microscope (TEM)

The size and morphology of nanoparticles were studied by Hitachi Transmission Electron Microscope Hi-7650 at an accelerated voltage of 200 kV by casting a drop of particle solution onto a 200-mesh carbon coated copper grid in EMN laboratory, Punjab Agricultural University, Ludhiana. TEM pictures obtained were employed in ImageJ software to study particle size distribution of nanoparticles and for each nanoparticle under analysis, diameter was determined and average size was calculated.

ii. Scanning Electron Microscope (SEM)

Scanning electron micrographs of prepared nanoparticles were recorded using SEM model Hitachi S-3400 in EMN laboratory, Punjab Agricultural University, Ludhiana.

iii. Dynamic Light Scattering (DLS)

Particle size distribution analysis of nanoparticles was carried out using Litesizer 500 in Application Lab, Anton Paar, Gurgaon, India.

iv. Zeta potential analysis

Zeta potential of nanoparticles was determined using Litesizer 500 in Application Lab, Anton Paar, Gurgaon, India.

v. UV-Visible analysis

Absorption spectra of prepared samples were recorded using UV-1800 Shimadzu Double-Beam Spectrophotometer in the wavelength range of 200-800nm.

vi. Infrared (IR) Spectroscopy:

The IR spectra were recorded on Alpha Bruker-2 in our lab.

3.1 Synthesis of silver sulfide nanoparticles (Ag_2S NPs)

3.1.1 Synthesis of silver sulfide nanoparticles (Ag_2S-1 NPs) using thiourea ($SC(NH_2)_2$)

Silver nitrate (0.0095 g, 0.0003 M) was dissolved in 200 ml distilled water in 250 ml round bottom flask. In another 250 ml flask, thiourea (0.0045 g, 0.0003 M) was dissolved in 200 ml distilled water. 20 ml of prepared silver nitrate solution (0.0003 M) with 2-3 drops of diluted triton-X as a surfactant was taken in a flask to which 10 ml of thiourea solution (0.0003 M) was added dropwise while sonication to obtain a light yellow coloured solution. The solution was irradiated with microwave radiations for 25 seconds and allowed to cool down at the room temperature. PVP (0.03 g) dissolved in 5 ml distilled water, was added to above prepared solution during sonication which acted as stabilizing agent. The sonication was further contiuned for 15 minutes to get PVP stabilized Ag_2S-1 NPs in aqua dispersed form (49.56 ppm).

3.1.2 Synthesis of silver sulfide nanoparticles (Ag_2S-2 NPs) using thioaceteamide (CH_3CSNH_2)

Thioacetamide (0.0045 g, 0.0003 M) was dissolved in 200 ml distilled water in 250 ml round bottom flask. Silver nitrate solution (20 ml, 0.0003 M) with 2-3 drops of diluted triton-X was taken in a flask and 10 ml of thioacetamide solution (0.0003 M) was added dropwise into it under sonication, resulting in light yellow in coloured solution. The solution was further irradiated with microwave radiations for 25 seconds and allowed to cool down at the room temperature. PVP (0.3 g) dissolved in 5 ml distilled water, was added to above prepared solution during sonication. The sonication was further continued for 15 minutes to PVP stabilized Ag_2S-2 NPs in aqua dispersed form (49.56 ppm)**.**

3.1.3 Synthesis of silver sulfide nanoparticles (Ag_2S-3 NPs) using Sodium thiosulfate pentahydrate

($Na_2S_2O_3.5H_2O$)

Sodium thiosulfate pentahydrate $Na_2S_2O_3.5H_2O$ (0.015 g) was dissolved in 200 ml distilled water in 250 ml of round bottom flask to get 0.0003 M solution. 20 ml of prepared silver nitrate solution with 2-3 drops of diluted triton-X as a surfactant was taken in flask and 10 ml of Sodium thiosulfate pentahydrate solution (0.0003 M) was added dropwise into it under sonication. The obtained solution was light yellow in colour. The solution was further irradiated with microwave radiations for 25 seconds and allowed to cool down at the room temperature. PVP (0.3 g) dissolved in 5 ml

distilled water, was added to above prepared solution during sonication, acting as stabilizing agent. The sonication was further continued for 15 minutes to PVP stabilized aqua dispersed Ag_2S-3 NPs (49.56 ppm).

3.1.4 Synthesis of silver sulfide nanoparticles (Ag_2S-4 NPs) using sodium sulfide (Na_2S)

Sodium sulfide (0.0045 g) was dissolved in 200 ml distilled water in 250 ml round bottom flask to get 0.0003 M solution. In another flask, 20 ml of prepared silver nitrate solution (0.0003 M) along with a drop of triton-X was taken and 10 ml of sodium sulfide solution was added dropwise during sonication. The light yellow solution was obtained. The solution was allowed to cool down at the room temperature. PVP solution (0.3 g/5 ml) was added to above prepared solution during sonication, which was continued for another 15 minutes to get aqua dispersed PVP stabilized Ag_2S-4 NPs (49.56 ppm).

3.2 Synthesis of silver nanoparticles (Ag NPs)

Silver nanoparticles were synthesized by means of chemical reduction method, using sodium borohydride as a reducing agent (Aashritha 2013). A 10-ml volume of 1.0 mM silver nitrate was added dropwise (about 1 drop per second) to 10 ml of 5.0 mM sodium borohydride solution containing 1drop of Triton X, while stirring, in ice cold conditions. The solution turned light yellow after the addition of silver nitrate which was primary indication for the synthesis of silver nanoparticles (Nasrollahi 2011). The chemical reaction involving the chemical reduction of aqueous solution of silver nitrate using sodium borohydride is given as:

$$AgNO_3 + NaBH_4 \longrightarrow Ag + 1/2\ H_2 + 1/2\ B_2H_6 + NaNO_3$$

0.1g of polyvinyl pyrollidone K-30 dissolved in 5 ml of distilled water was added to synthesized silver nanoparticles. The solution was centrifuged at 10,000 rpm for 10 min and was resuspended in same amount of double distilled deionised water. This resulted in stable 0.5 mM solution of PVP-coated silver nanoparticles which was analysed and confirmed on the basis of UV–visible and TEM analysis.

3.3 Synthesis of chitosan decorated Ag_2S NPs

Chitosan nanoparticles were prepared by dissolving 75 mg of chitosan in 5 ml of glacial acetic acid. The mixture of chitosan and glacial acetic acid was stirred for 2 hours at 80ºC to make chitosan completely soluble in acetic acid. The above solution after stirring, was added to 245 ml of distilled water while sonication, which was continued for 30 min to get chitosan nanoparticles (300 ppm).

During sonication, 20 mg of $AgNO_3$ and 5 mg of Na_2S was added to the above prepared solution to to get chitosan decorated Ag_2S NPs nanoparticles (1:2 molar

ratio). The active concentrations of chitosan NPs and Ag_2S NPs were 300 ppm and 600 ppm, respectively.

3.4 Screening of antifungal activity

The synthesized Ag_2S NPs, Ag NPs and chitosan decorated Ag_2S NPs nanoparticles were screened *in vitro* for their antifungal potential against four test fungi *viz. Ustilago hordei*,*Uromyces viciafabia*, *Fusarium moniliforme and Bipolaris oryzae* by spore germination and poisoned food technique. The results have been expressed in terms of ED_{50} values *i.e.* the effective dose at which 50 percent inhibition has occurred.

3.4.1 Source

The diseased samples of the four test fungi were collected from experimental areas of Punjab Agricultural University, Ludhiana and were causing the following disease:

Fusarium moniliforme –It is the most commonly known fungal species of rice. It causes foot rot in rice. Tilt is commercially used as a standard fungicide against *F. moniliforme* with ED_{50} value of 25 µg/ml.

Bipolaris oryzae– It is the causal agent of rice brown spot disease. In order to control this disease, Captan is commencially used as an effective antifungal agent against *B. oryzae* which have ED_{50} value of approximately 35µg/ml.

Ustilago hordei– False smut of rice is caused by *Ustilago hordei*. The appearance of *U. hordei* is generally observed as covered smut of Barley. To prevent this disease, Carboxin can be used as a standand fungicide. The ED_{50} value of Carboxin against *U. hordei* is 78 µg/ml.

Uromyces viciafabia – It causes rust on broad stems and leaves of pea which results in partial defoliation of the crop. Carboxin (ED_{50} = 70 µg/ml) is reported as an effective antifungal agent to control the infection caused by *U. viciafabia.*

3.4.2 Isolation and maintenance

Diseased sample were washed in running tap water for 5-10 minute. The infected parts were cut into small pieces with the help of sterilized blade. They were sterilized by dipping them into mercuric chloride solution (0.1%) for one minute and further washed with sterilized distilled water for three times. The sterilized diseased pieces were shifted to potato dextrose agar (PDA) media (200 g small pieces of peeled potato, 20 g agar and 20 g dextrose in 1 litre distilled water) slants under aseptic environment. These test tubes were incubated at 25±1°C in case of *Fusarium moniliforme and Bipolaris oryzae* in order to obtain good development of test fungi. The cultures, thus obtained, were decontaminated and preserved by further sub culturing on PDA slants which were then stored in the refrigerator.

3.4.3 Preparation of silver sulfide nanoparticles stock solution

All the Ag_2S NPs stock solutions were diluted to 30 ppm, 20 ppm, 15 ppm, 10 ppm and 5ppm using normality equation, as and when required. Corresponding standard were also dilute from high concentration to low concentration as per the requirement.

3.4.4 Spore Germination Inhibition Technique: *Ustilago hordei* and *Uromyces viciafabia* were evaluated by spore germination inhibition technique. A drop of spore suspension (0.02 ml) in equal quantity with solution of test compound will be seeded in the cavities of cavity slides. The slides will be placed in Petri plates lined with moist filter paper and will be incubated at 25±1ºC. The germination of spores will be recorded at regular intervals of 24 hours and the per cent spore germination inhibition will be calculated by the following formula:

$$\text{Percent spore germination inhibition} = \frac{C - T}{C} \times 100$$

Where, C = Spore germination in control

T = Spore germination in treatment

The antifungal activity will be expressed in terms of ED_{50} values.

3.4.5 Procedure for preparation of Potato dextrose agar (PDA)

Peeled potatoes (200 g) were boiled in 1000 ml of distilled water with the help of a cooker for 20 minutes. After 20 minutes, 20 g of agar agar and 20 g of dextrose was added in the solution. The mixture was boiled with continuous stirring until the agar agar and dextrose was completely dissolved in the solution. The total volume was made to one litre with distilled water. PDA solution of 99 ml was poured into sterilized conical flasks (250 ml) and was plugged with non-absorbent cotton wool. The flasks were arranged, covered with a paper sheet and were sterilized in an autoclave at 15 psi (121 °C) for 20 minutes. The sterilized flasks were taken out after releasing the steam and cooled at room temperature.

Potato dextrose agar	
Peeled potatoes	200 g
Dextrose	20 g
Agar agar	20 g
Distilled water	1000 ml

3.4.6 Poisoned Food Technique: Antifungal activity against *Fusarium moniliforme* and *Bipolaris oryzae* was tested by poisoned food technique. Approximately 99 ml of Potato Dextrose Agar (PDA) media will be taken in the round bottom flasks, 1 ml with different concentrations of each compound will be added to different flasks and

the contents will be mixed thoroughly. The contents of the flask will be poured aseptically into the petriplates. Test compound however, will be replaced by an equal amount of PDA only in the control set. After the media will solidify one inoculum disc of mycelium of the test fungus, will be aseptically placed or will be inoculated to each Petri plate and will be incubated at 24±1˚C. The average diameter of fungal colonies will be measured upto 7 days after inoculation.

The percent inhibition in growth will be calculated by using following formula:

$$\text{Percent inhibition} = \frac{C - T}{C} \times 100$$

Where, C = Radial growth in control

T = Radial growth in treatment

The antifungal activity will be expressed in terms of ED_{50} values.

CHAPTER-IV

RESULTS AND DISCUSSION

4.1 Characterization of silver sulfide nanoparticles (Ag_2S NPs)

Silver sulfide nanoparticles (Ag_2S NPs) in aqua-dispersed form were synthesized using sonochemical irradiation method. Silver ions were allowed to interact with different sulfide ion sources, while sonication. Thiourea ($SC(NH_2)_2$), thioacteamide (CH_3CSNH_2), sodium thiosulfate pentahydrate ($Na_2S_2O_3.5H_2O$) and sodium sulfide (Na_2S) were different sulfide sources used. The change in colour from transparent to pale yellow indicated the formation of Ag_2S NPs in aqua-dispersed form. These dispersed nanoparticles were stabilized using polyvinyl pyrollidone (PVP). The prepared samples of Ag_2S NPs were characterized by Transmission Electron Microscopy (TEM), UV-Visible Spectroscopy (UV-Vis), Fourier Transform Infra-red Spectroscopy (FTIR), Dynamic Light Scattering (DLS), Zeta potential, Scanning Electron Microscopy (SEM) and Energy Dispersive Spectroscopy (EDS).

Particle size and optical properties

The particle size of synthesized Ag_2S NPs in aqua-dispersed form was studied by TEM morphographs which indicated perfectly spherical shaped nanoparticles in all cases except Ag_2S-1(Fig. 1-4) where distorted spherical shape with slight aggregation was observed. The particle sizes ranged from 10-20 nm. The least size was observed in case of Ag_2S-4 NPs (Fig. 4) which was 10±1 nm while in case of Ag_2S-2 (Fig. 2) maximum size was observed to be 20±1 nm. The average sizes of all prepared samples are given in Table 1, which was in consonance with the reported literature (Kuznetsova *et al* 2017, Han *et al* 2012, Kumar *et al* 2015, Kim *et al* 2010) where the sizes varied from 9-20nm.

UV-Vis studies were performed by measuring the absorbance of the aqua-dispersed Ag_2S NPs in the 200–800 nm region. The maximum absorption between 270-295 nm (Fig. 5) indicated the presence of Ag_2S NPs (Xaba *et al* 2017). The λ_{max} of Ag_2S NPs was in good agreement with the previously reported optical properties of Ag_2S NPs (Kuznetsova *et al* 2017).

Optical properties of the Ag_2S NPs were measured in freshly prepared dispersions as well as and in the same dispersions after regular intervals of 15 days till 4 months. There were no significant diversions from the starting values revealing long shelf life of prepared nanoparticles.

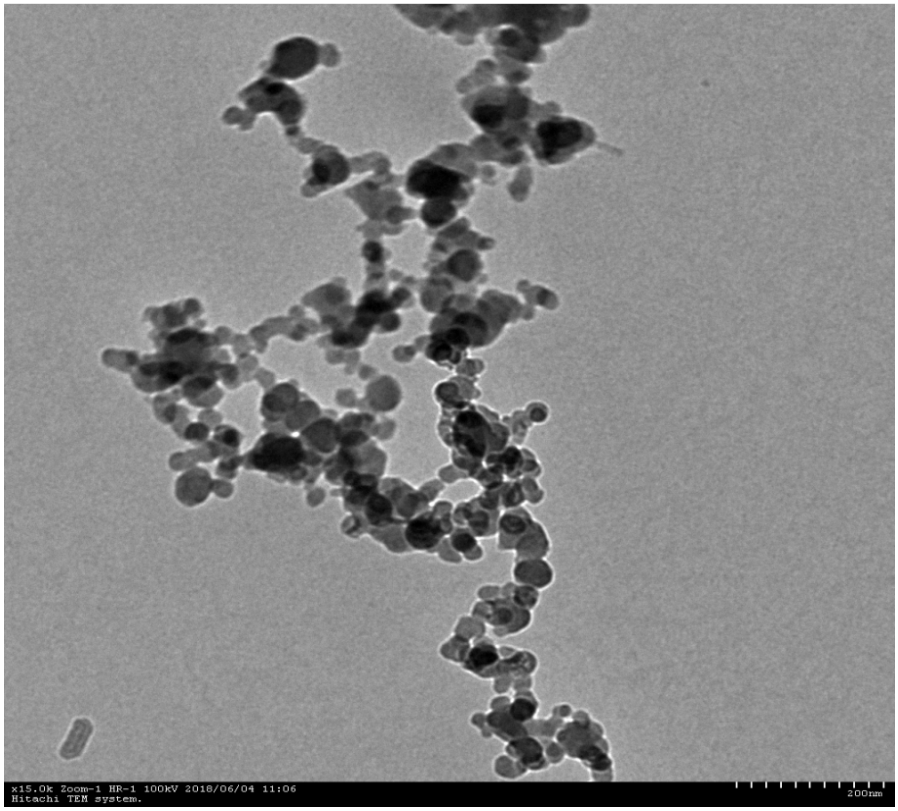

Fig. 1 TEM image of sample Ag_2S-1 NPs

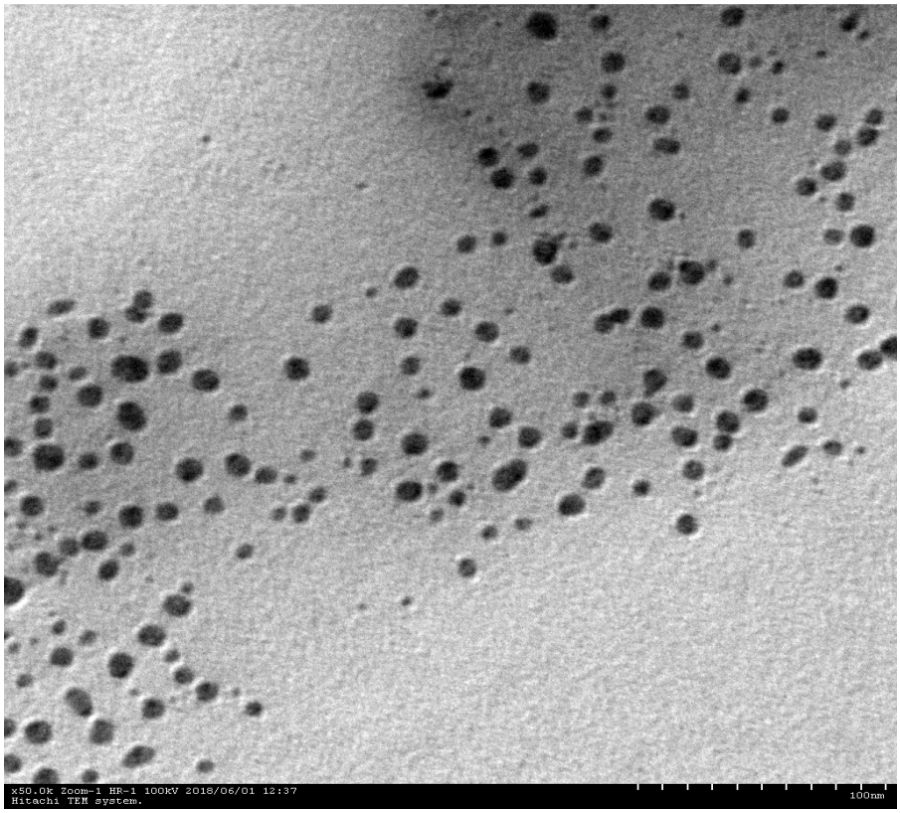

Fig. 2 TEM image of sample Ag_2S-2 NPs

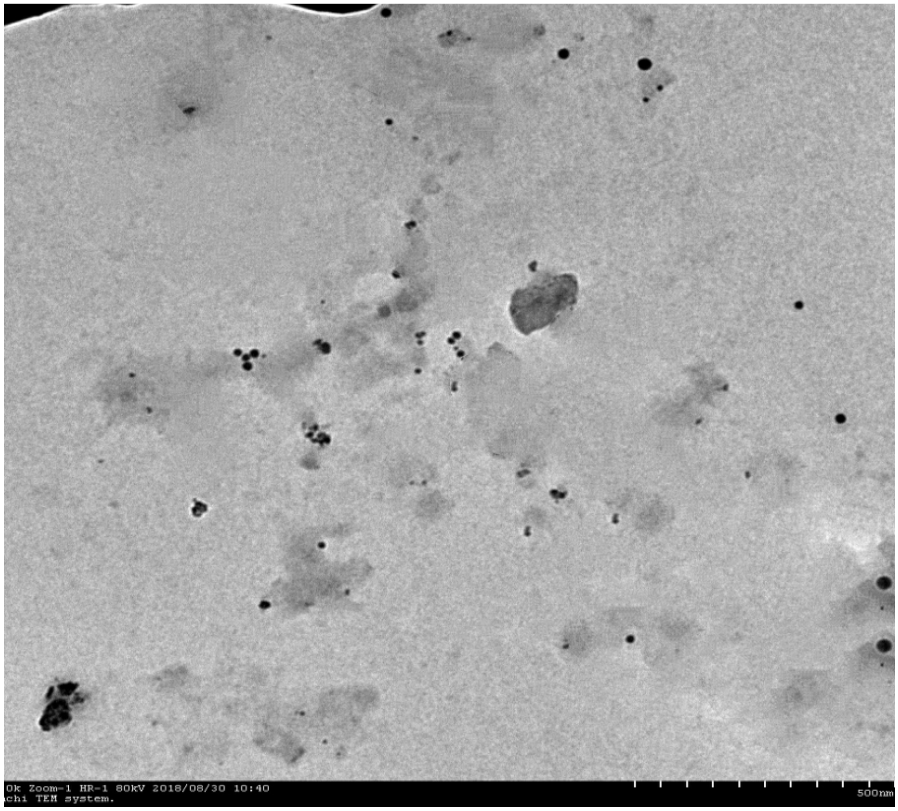

Fig. 3 TEM image of sample Ag_2S-3 NPs

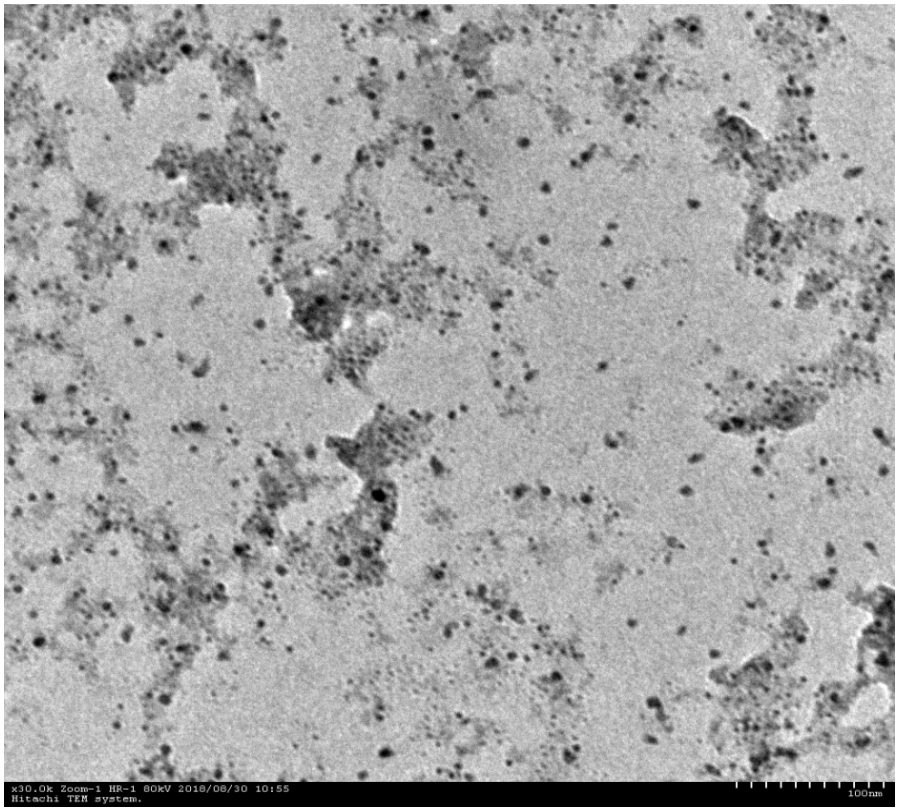

Fig. 4 TEM image of sample Ag_2S-4 NPs

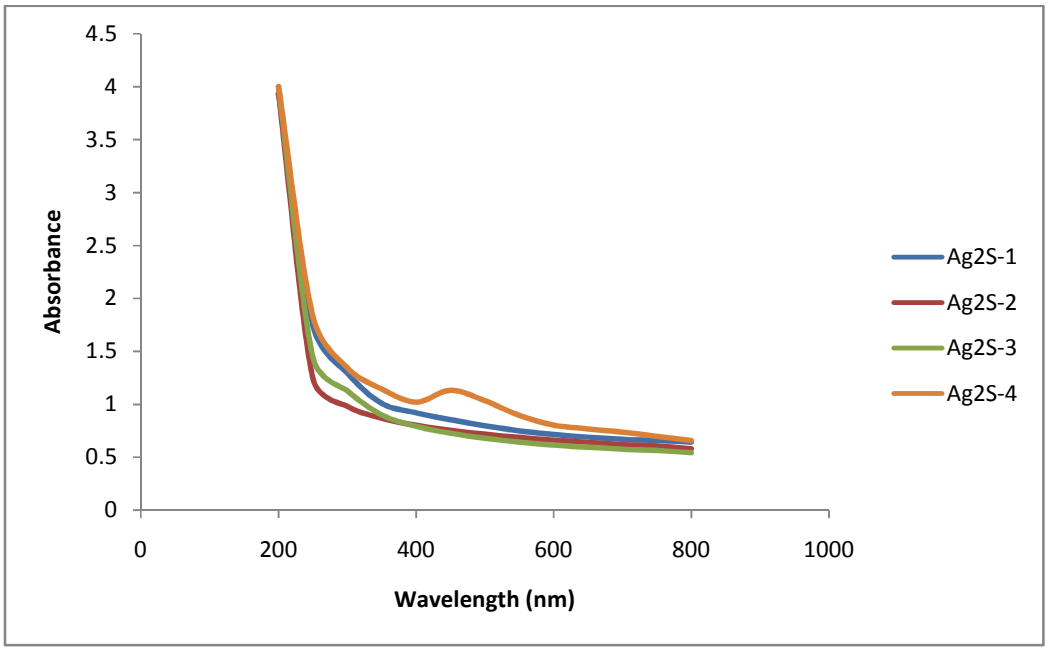

Fig. 5 UV-Vis spectra Ag_2S NPs

Table 1. Size and Optical properties of synthesized silver sulfide NPs

Sample No.	Sulfide ion source	λ_{max}(nm)	Average size (nm)
Ag_2S-1	Thiourea	279	18±2
Ag_2S-2	Thioacetamide	295	20±1
Ag_2S-3	Sodium thiosulfate pentahydrate	273	11±3
Ag_2S-4	Sodium sulfide	270	10±1

SEM-EDS analysis

SEM-EDS were explored to test the surface appearance, particle morphology and elemental composition of Ag_2S NPs. The SEM-EDS spectrum confirmed the presence of silver and sulfur in the elemental ratio of 2:1. The SEM micrograph of sample Ag_2S-1 revealed spherical morphology and their elemental composition showed by EDS spectra was 34.46 % S and 65.54 % Ag. The micrograph of sample Ag_2S-2and Ag_2S-3 showed a wire like structure and sample Ag_2S-4 showed that the particles were spherical and smooth in nature and the EDS spectrum confirmed the presence of sulfur and silver in elemental ratio of (32.57% S, 67.43%Ag), (33.17% S and 66.83% Ag) and (33.89 % S, 66.11%Ag), respectively (Fig. 6-9).

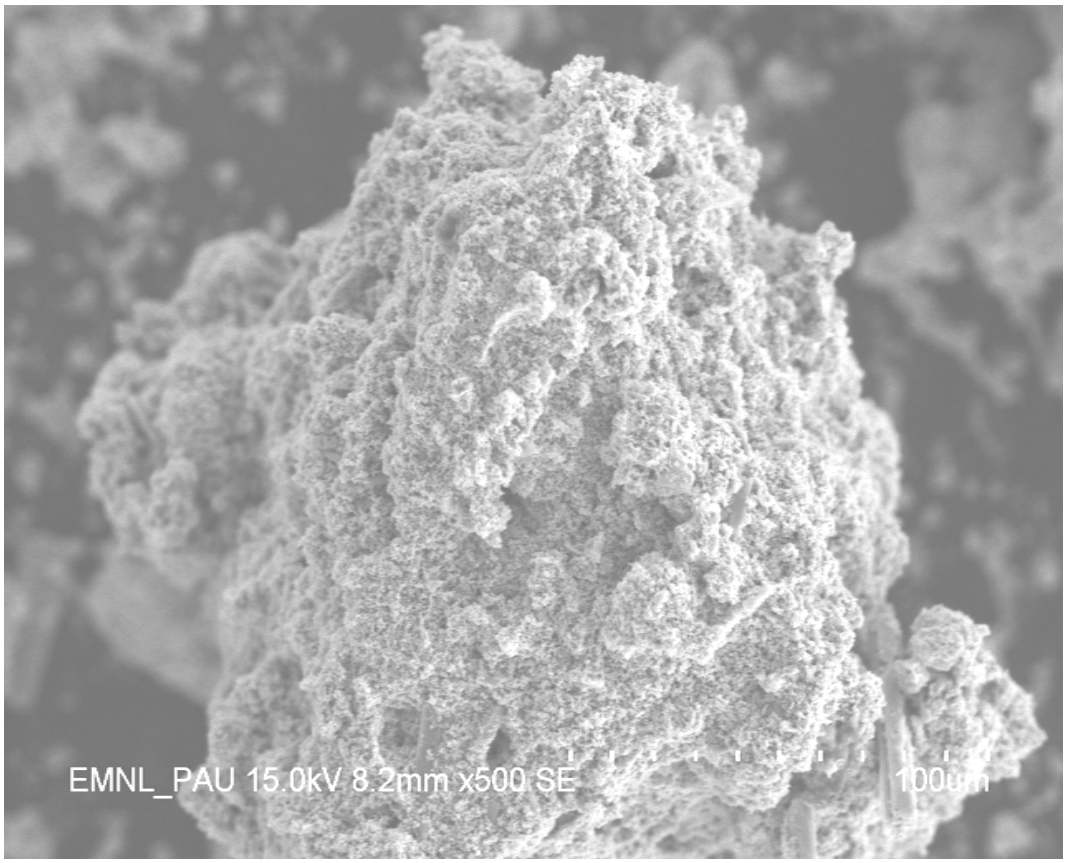

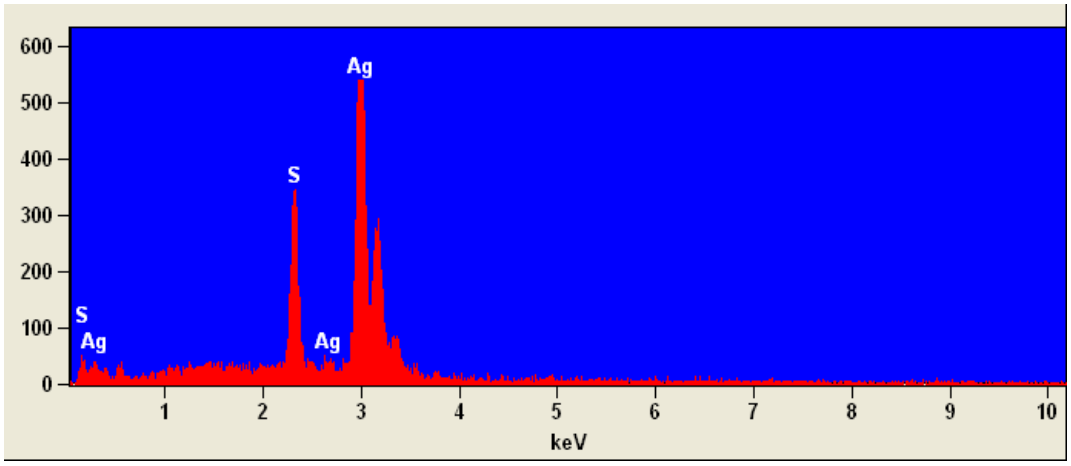

Fig. 6 SEM image and EDS spectrum of Ag_2S-1NPs

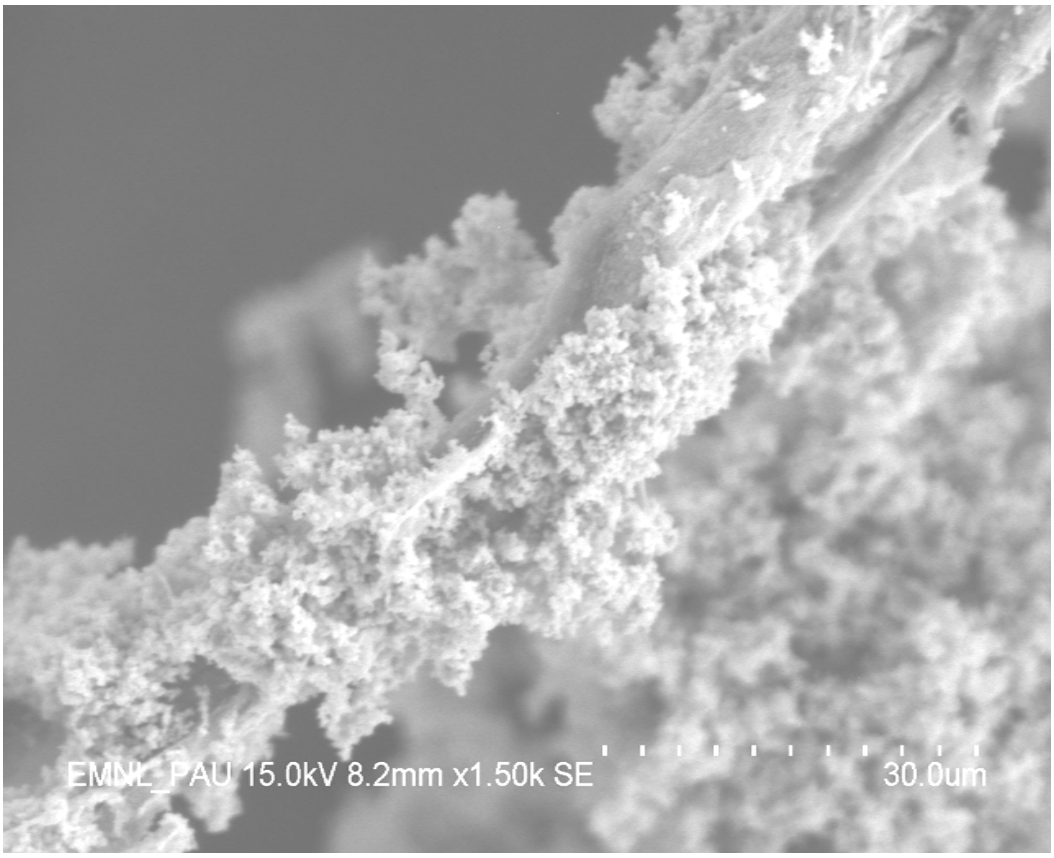

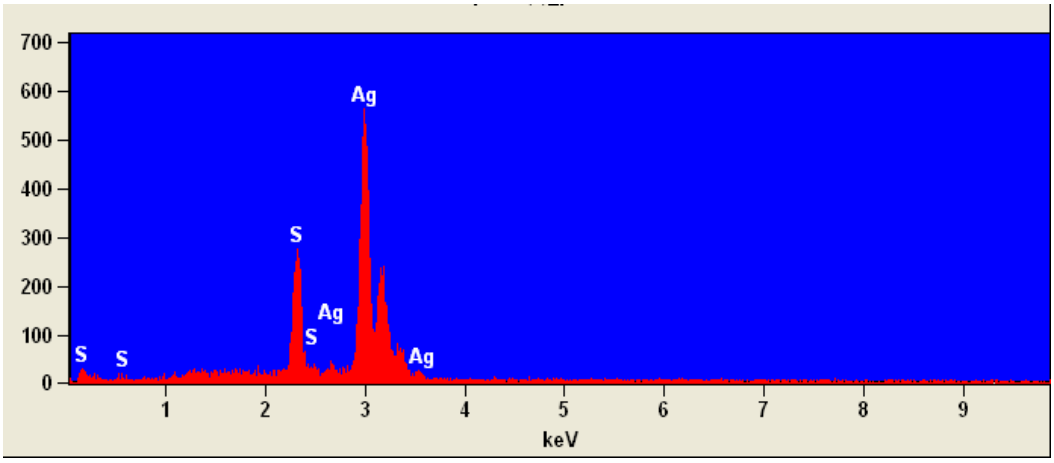

Fig. 7 SEM image and EDS spectrum of Ag_2S-2 NPs

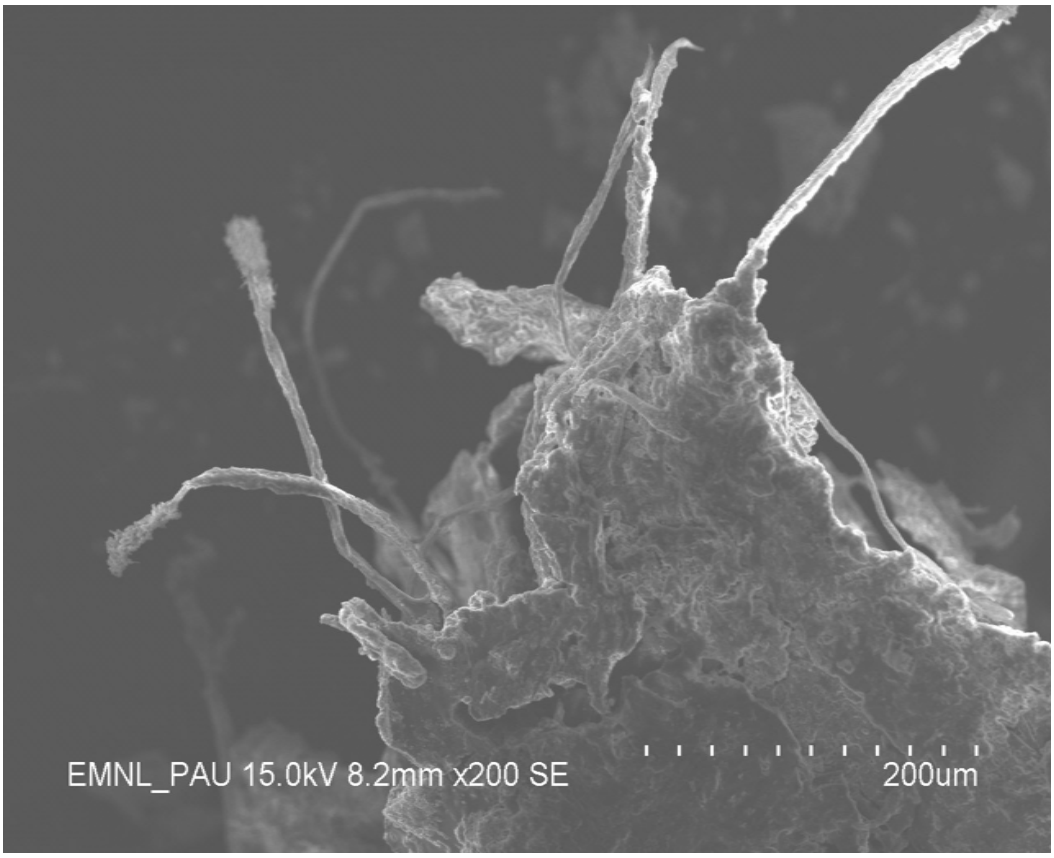

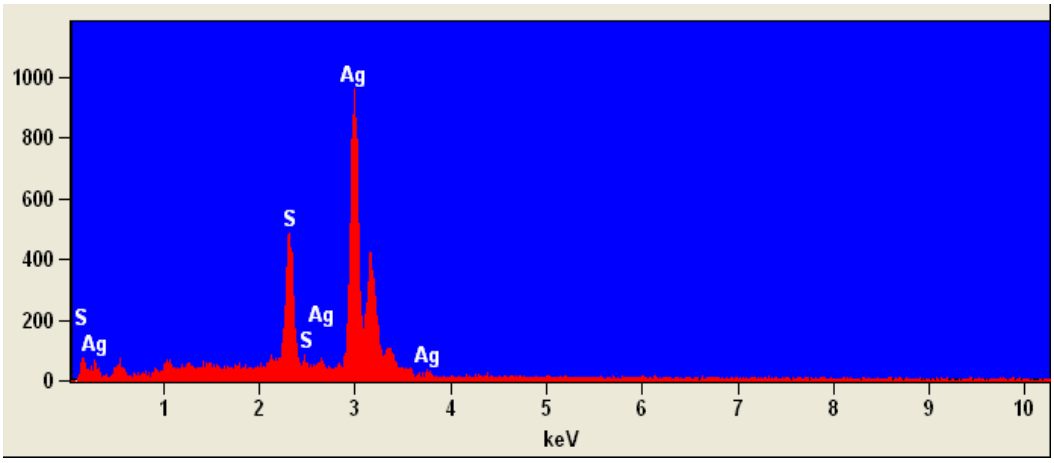

Fig. 8 SEM image and EDS spectrum of Ag_2S-3 NPs

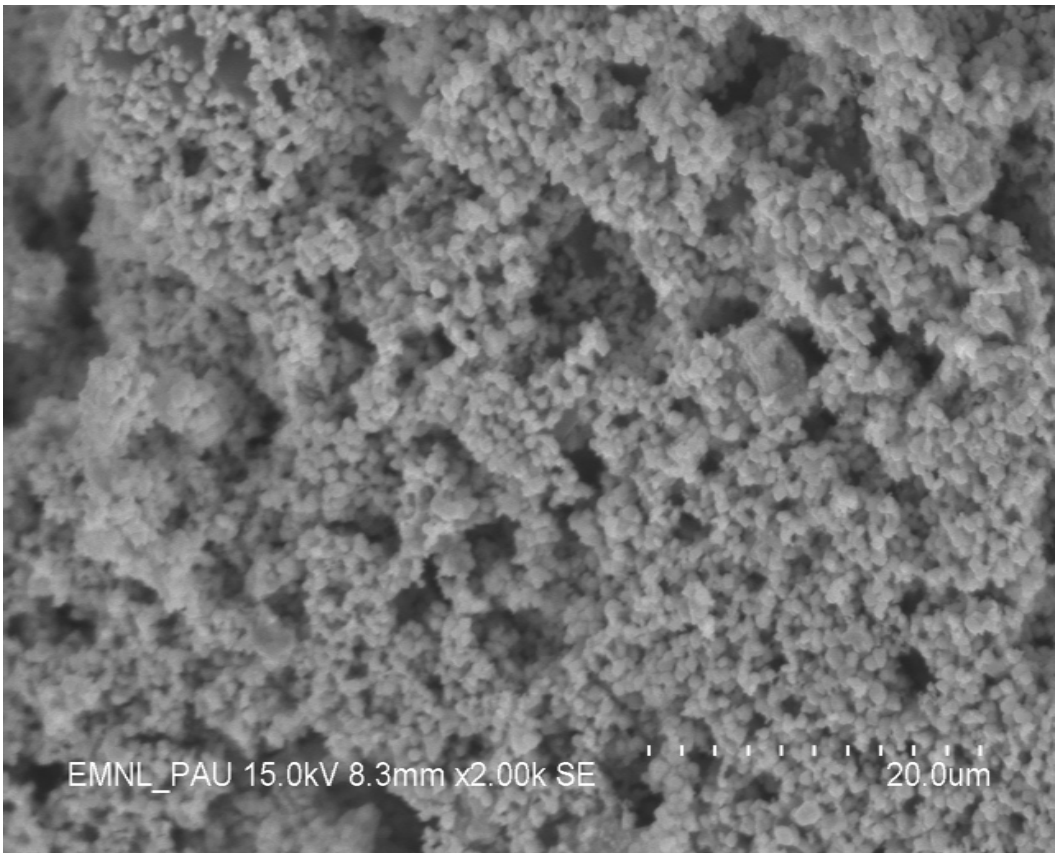

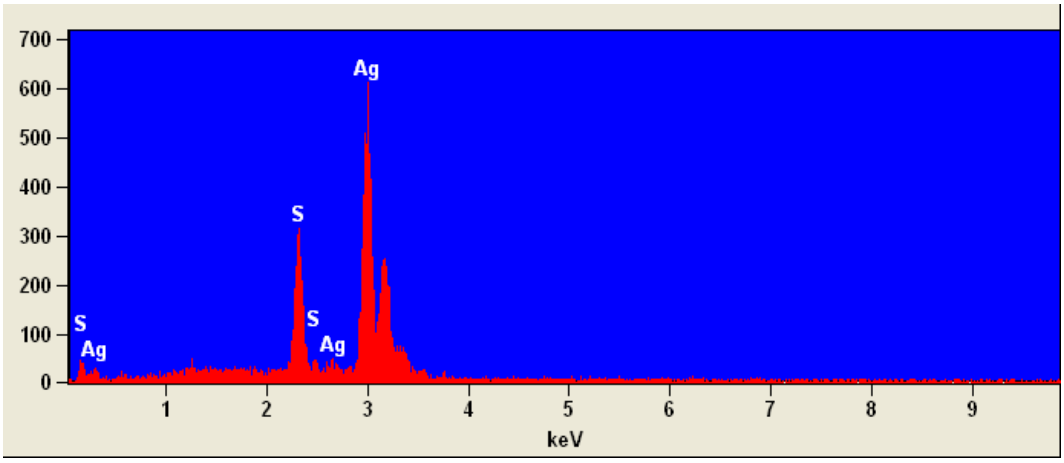

Fig. 9 SEM image and EDS spectrum of Ag_2S-4 NP

Dynamic light scattering (DLS)

Dynamic light scattering (DLS) is the second main method of particle size determination. It is a method used to determine size distribution of nanoparticles in suspensions. The DLS instrument shows the results as a size distribution by intensity. From this distribution, the Z-average size is calculated by the instrument. Z-average is

the mean size as weighed by intensity. The DLS size distribution of synthesized silver sulfide nanoparticles **Ag_2S-(1-4)** exhibited hydrodynamic diameter of 224.7 nm, 228.4 nm, 143.74 nm and 113.25 nm respectively (Fig. 10-13). DLS showed results of the mean diameter in the higher end of the size distribution obtained by TEM. The particle size, which is derived from the DLS measurement, is not the true size, but rather this method considers solvation layer around the particle to be a part of it. Because of this, the particles, when measured using DLS, look bigger, than their actual size. Also larger particles tend to cover smaller ones, so, the DLS measurement is quite broad.

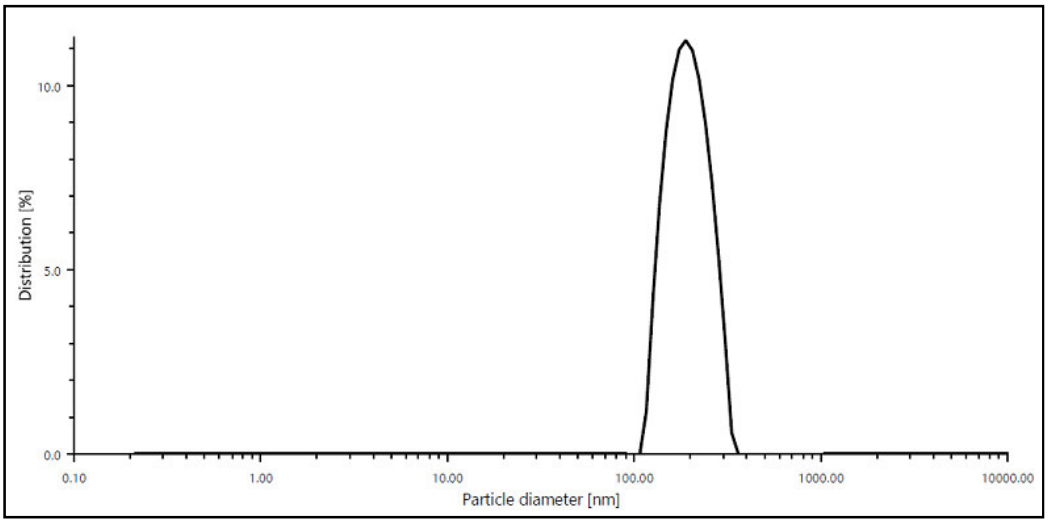

Fig. 10 DLS particle size distribution of Ag_2S-1NPs

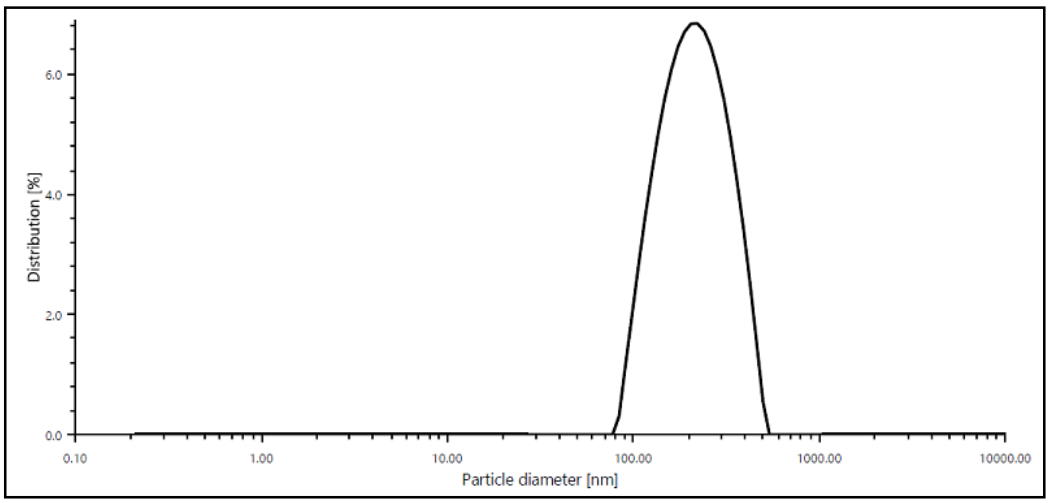

Fig. 11 DLS particle size distribution of Ag_2S-2 NPs

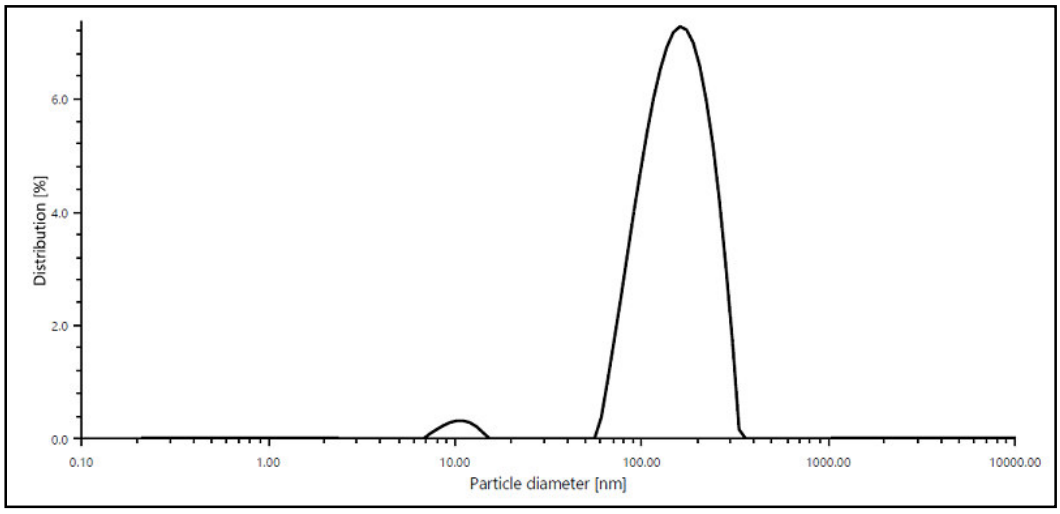

Fig. 12 DLS particle size distribution of Ag_2S-3 NPs

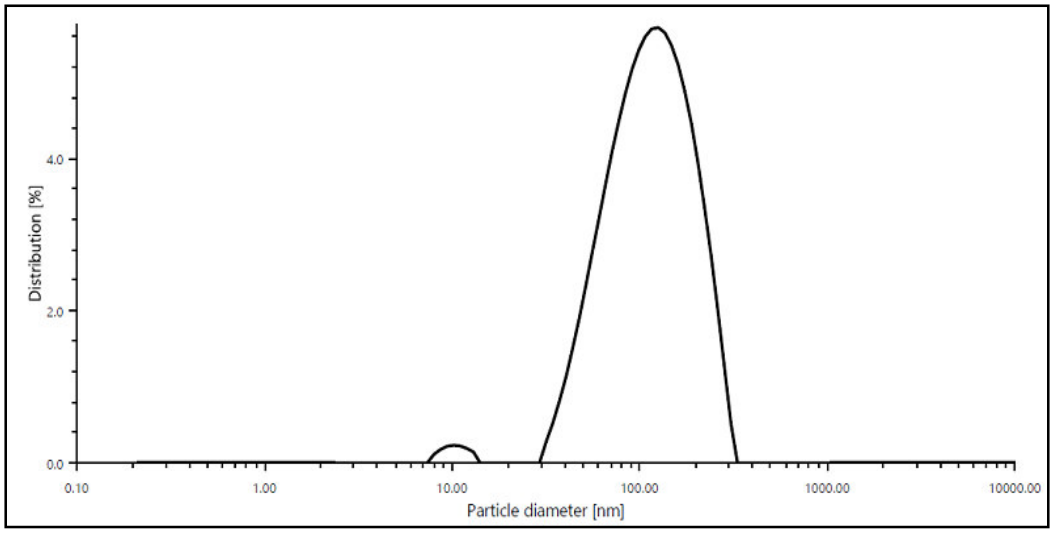

Fig. 13 DLS particle size distribution of Ag_2S-4NPs

Zeta potential

The zeta potentials of **Ag_2S-1**, **Ag_2S-2**, **Ag_2S-3 and Ag_2S-4**were -14.6 mV, -12 mV, -13.7 mV and -16.2 mV (Fig. 14-17) respectively. This negative value of zeta potential confirmed the presence of net negative charge on the surface of nanoparticles and high repulsions among the particles, which will prevent the coagulation of particles and leads to the formation of stable Ag_2S NPs.

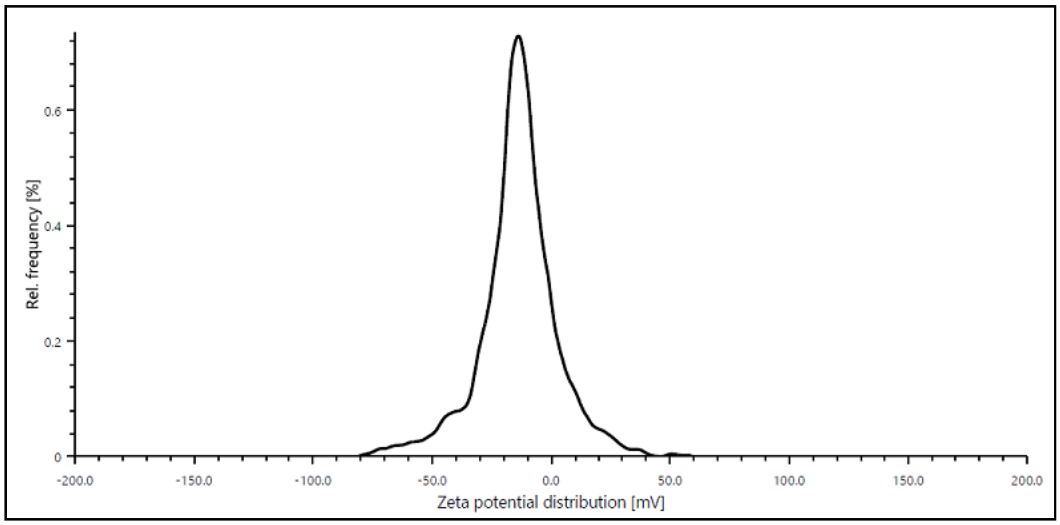

Fig. 14 Zeta potential of Ag_2S-1NPs

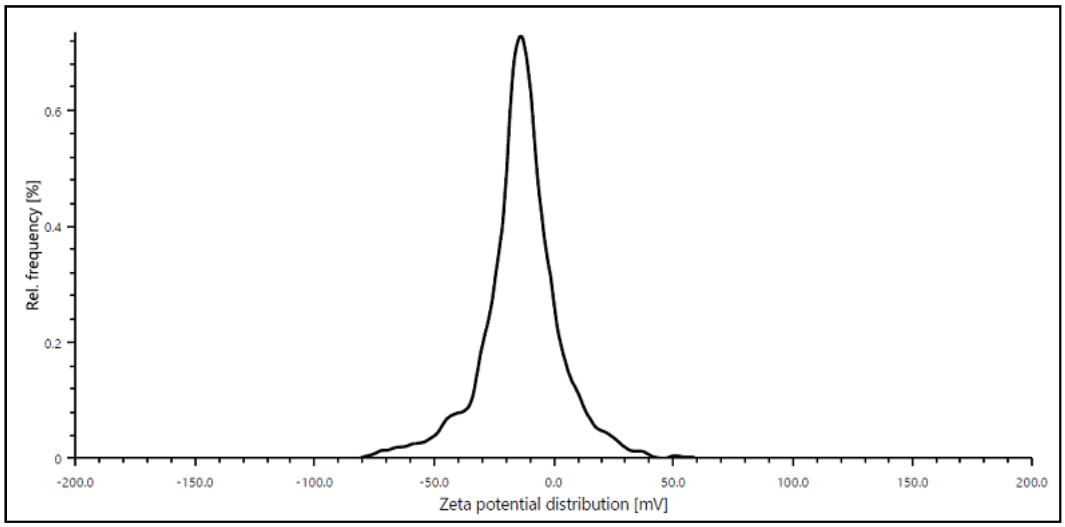

Fig. 15 Zeta potential of Ag_2S-2 NPs

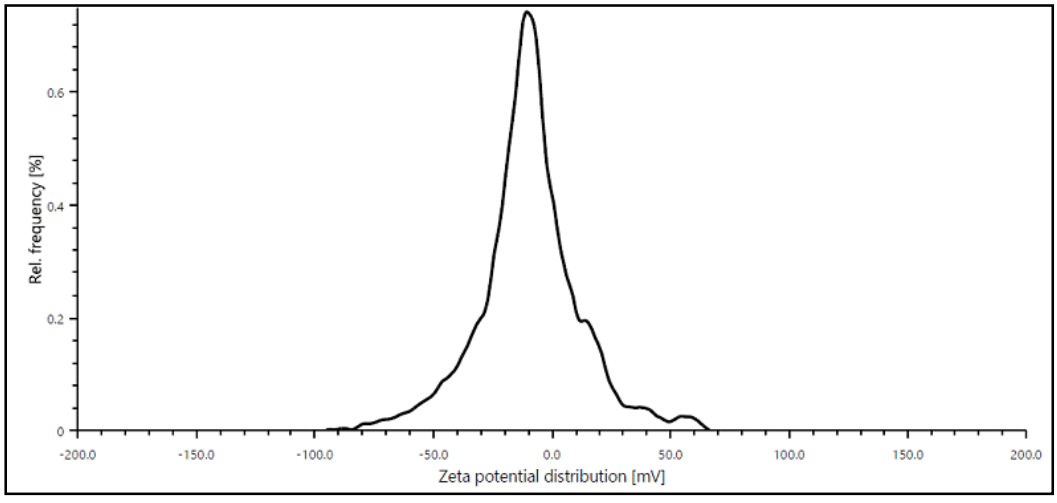

Fig. 16 Zeta potential of Ag_2S-3 NPs

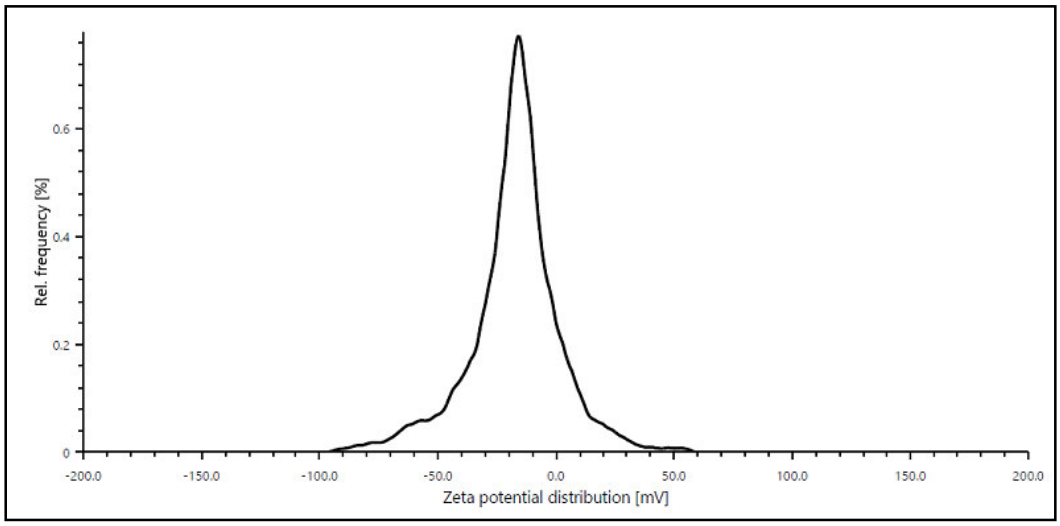

Fig. 17 Zeta potential of Ag_2S-4NPs

4.2 Characterization of Ag NPs

Typical chemical reduction methodology was used for the synthesis of silver nanoparticles (Ag NPs) using silver nitrate as source of silver and sodium borohydride as reducing agent with Triton X as surfactant, in ice cold conditions. The morphology and particle size Ag NPs was studied by transmission electron microscopy (TEM). TEM micrograph (Fig. 18) depicted that prepared naked nanoparticles were in spherical shape and uniformly distributed without any agglomeration with diameter in range of 8.6-8.8 nm (Fig. 19). In UV–Vis spectra a very pronounced plasmon absorption band of naked silver nanoparticles appeared at 412 nm (λ max) characteristic of a silver colloid as represented by curve in Fig 20.

4.3 Characterization of chitosan decorated Ag_2S NPs

TEM analysis indicated that the particle size of naked Ag_2S NPs was 10±1 nm, whereas the DLS size was 113.25 nm. The DLS size distribution was quiet larger than the TEM size due the involvement of solvation layer around the particles. From the optical studies the maximum absorption of naked Ag_2S NPs was observed at 267 nm, which correlated with the results of Xaba *et al* 2017.

The chitosan nanoparticles were prepared (Lotfi *et al* 2019) and conjugated with Ag_2S NPs. TEM image (Fig. 21) showed a thin coating of chitosan nanoparticles over Ag_2S NPs. The average diameter of chitosan coated Ag_2S NPs was 26±1 nm (Fig. 22). The average diameter of conjugate was comparatively more than Ag_2S NPs, due to the presence of extra coated layer of chitosan.

The IR data of chitosan decorated Ag_2S NPs indicated no significant shift or disappearance or appearance of the absorption bands relative to pure chitosan revealing no covalent bond formation in nanohybrids of chitosan with Ag_2S NPs. Chitosan have hard nitrogen and oxygen centres, which have poor interaction with

soft silver nanocores, therefore, only physical parameters are involved in the nanoconjugation of chitosan on Ag_2S NPs (Annexure 1 (a) Chitosan decorated Ag_2S NPs and (b) Chitosan)

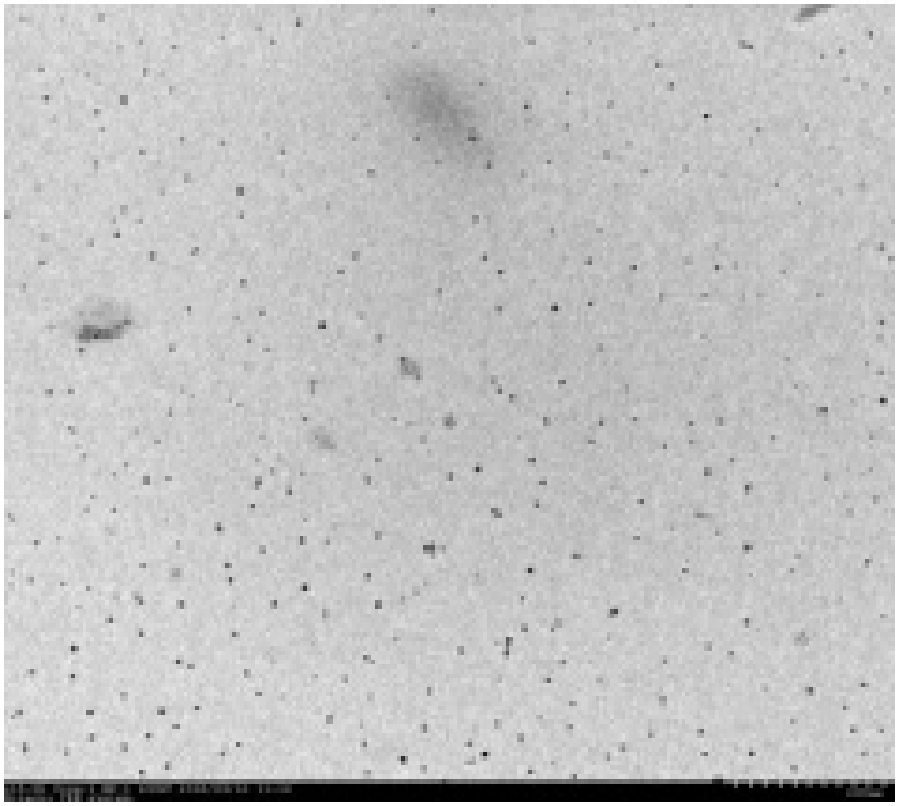

Fig.18 TEM analysis of unloaded AgNPs

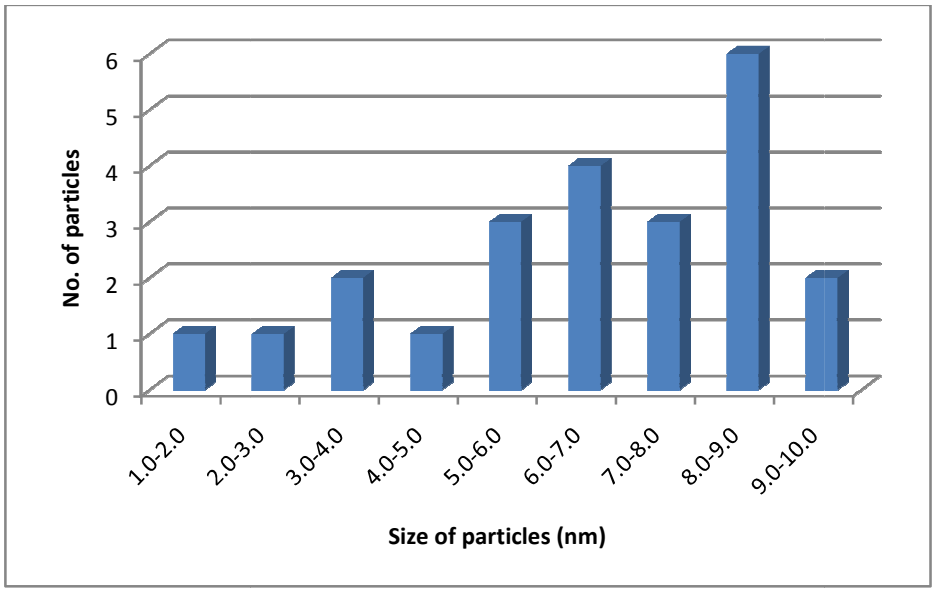

Fig.19 Particle size distribution of Ag NPs

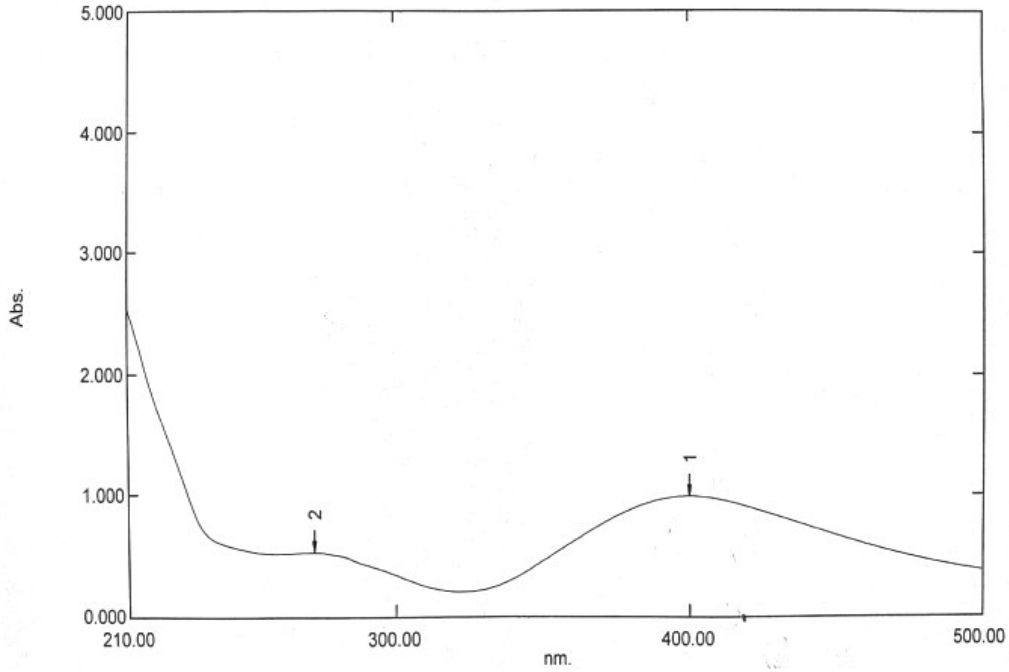

Fig.20 UV analysis of AgNPs

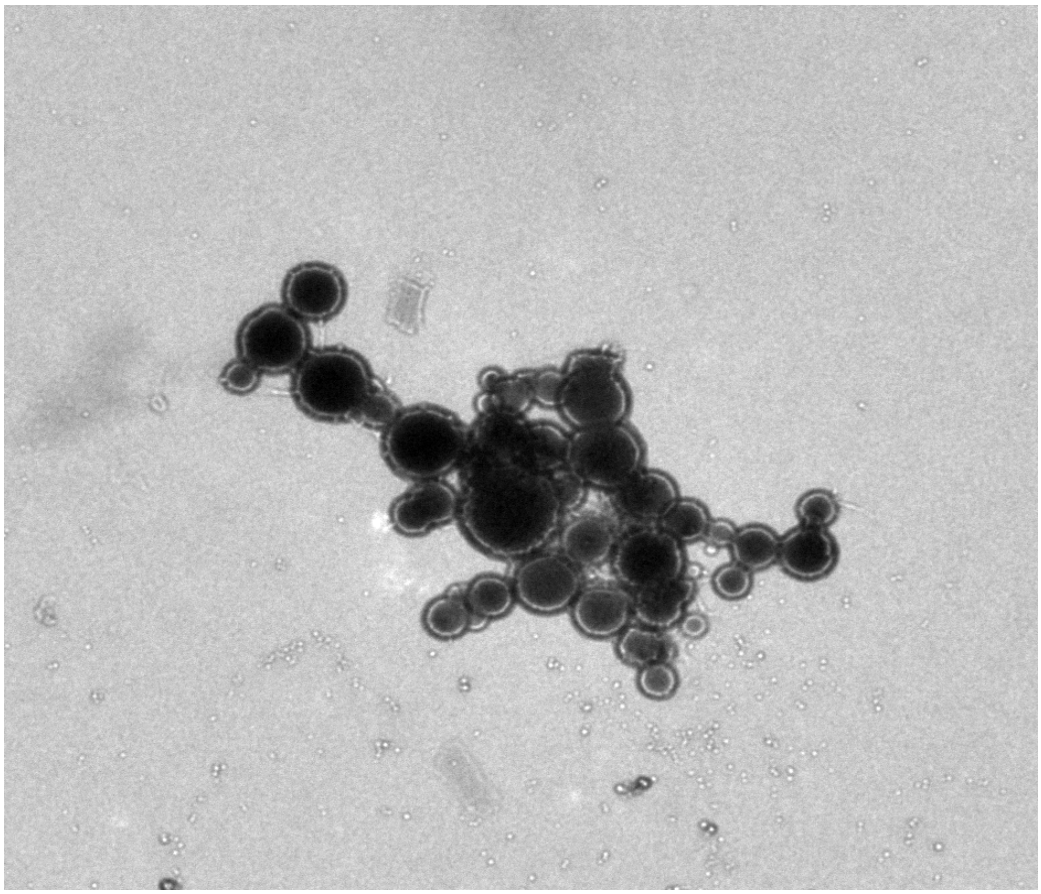

Fig. 21 TEM images of chitosan decorated Ag_2S NPs

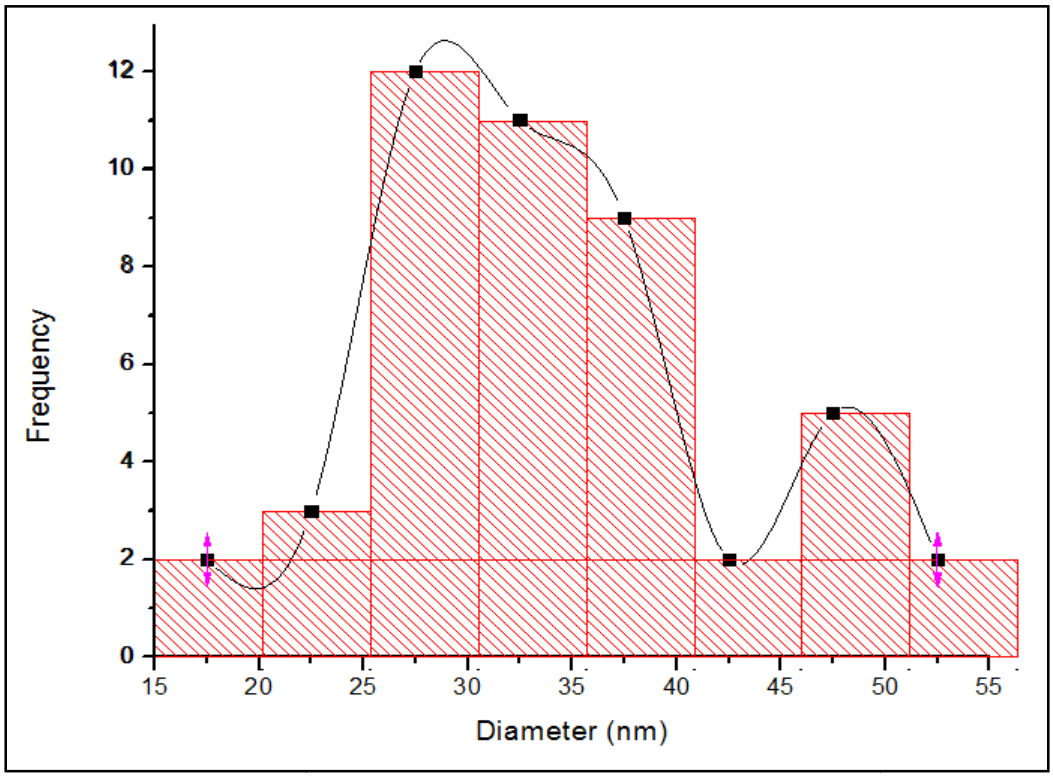

Fig.22 Particle size distribution of chitosan decorated Ag_2S NPs

4.4 Antifungal Activity of Aqua-dispersed Ag_2S-(1-4) NPs

4.4.1 Spore germination inhibition technique

The synthesized Ag_2S-(1-4) nanoparticles were screened *in vitro*, against *Ustilago hordei* and *Uromyces viciafabia* by spore germination inhibition technique. The effective dose was expressed in terms of ED_{50} values at which 50 per cent inhibition occurred (Table 2) and percent inhibition at different concentrations was also evaluate. The mean of three replicate tests performed for each antifungal test, calculated using Analysis of Variance (ANOVA).

4.4.1.1 *U. hordei*

All prepared Ag_2S-(1-4) NPs in aqua-dispersed form were tested against *U. hordei* and were found to be effective with ED_{50} values less than 12 µg/ml (Table 3) in all of the cases, which was multi fold lower than the standard fungicide carboxin (ED_{50}= 78 µg/ml). The sample prepared using sodium sulfide i.e. Ag_2S-4 was found to be more active than the other three synthesized samples. The ED_{50} value of Ag_2S-4 was 8µg/ml. The treatments for Ag_2S-1, Ag_2S-3 and Ag_2S-2, Ag_2S-4 were non-significant by Tukey mean test.

4.4.1.2 *U. viciafabia*

All prepared Ag_2S-(1-4) NPs in aqua-dispersed form were tested against *U. viciafabia* and were found to be effective with ED_{50} values less than 15 µg/ml (Table

4) in all of the cases, which was multi fold lower than the standard fungicide carboxin (ED_{50}= 70 µg/ml). The sample prepared using sodium sulfide i.e. Ag_2S-4 was found to be more active than the other three synthesized samples. The ED_{50} value of Ag_2S-4 was 11µg/ml. All the treatments were significant by the Tukey mean test.

4.4.2 Poisoned Food Technique

Antifungal potential of Ag_2S NPs against *Fusarium moniliforme* (Fig. 23-26) and *Bipolaris oryzae* (Fig. 28-31) was also studied using PDA method, whose ED_{50} values and percent inhibition values were also calculated (Table 5 and Table 6 respectively). All the samples were tested at various concentrations against these two fungi. The sample Ag_2S-4 was found to be more active antifungal agent against both *Fusarium moniliforme* and *Bipolaris oryzae* with ED_{50} value at 11µg/ml and 13 g/ml respectively. The ED_{50} value of Ag_2S-4 was very less as compared to standard fungicides i.e. Tilt against *Fusarium moniliforme* (ED_{50}= 25 µg/ml) and Captan against *Bipolaris oryzae* (ED_{50}= 35 µg/ml). All the treatments against *Fusarium moniliforme* and *Bipolaris oryzae* were significant by the Tukey mean test.

4.5 Antifungal Activity of Ag NPs

4.5.1 Spore germination inhibition technique

The synthesized Ag NPs were screened *in vitro*, against *Ustilago hordei* and *Uromyces viciafabia* by spore germination inhibition technique. The effective dose was expressed in terms of ED_{50} values at which 50 per cent inhibition occurred (Table 2) and percent inhibition at different concentrations was also evaluate. The mean of three replicate tests performed for each antifungal test, calculated using Analysis of Variance (ANOVA).

4.5.1.1 *U. hordei*

The prepared sample of Ag NPs in aqua-dispersed form were tested against *U. hordei* and was found to be effective with ED_{50} values more than 18 µg/ml (Table 3). Thus we concluded that the Ag_2S NPs (ED_{50} < 12 µg/ml) were more effective antifungal agent against *U. hordei* than Ag NPs (ED_{50} > 18 µg/ml).

4.5.1.2 *U. viciafabia*

The prepared sample of Ag NPs in aqua-dispersed form were tested against *U. viciafabia* and was found to be effective with ED_{50} values more than 24 µg/ml (Table 4). Thus Ag_2S NPs with ED_{50} less than 15 µg/ml showed better antifungal activity against *U. viciafabia* in comparision to Ag NPs, whose ED_{50} value was more than 24 µg/ml. The treatment for the compound Ag NPS and carboxin were non-significant and the rest treatments were significant by Tukey mean test.

4.5.2 Poisoned Food Technique

Antifungal potential of Ag NPs against *Fusarium moniliforme* (Fig. 27) and *Bipolaris oryzae* (Fig. 32) was also studied using PDA method, whose ED_{50} values and percent inhibition values were also calculated (Table 5 and Table 6 respectively). The prepared sample was tested at various concentrations against these two fungi and was found to be an active antifungal agent against both *Fusarium moniliforme* and *Bipolaris oryzae* with ED_{50} value at 24 µg/ml and 27 µg/ml respectively (Table 2). The antifungal potential of Ag NPs was again very less as compared to Ag_2S NPs.

Table 2. Antifungal potential of aqua-dispersed Ag_2S-(1-4)NPs

Sample	ED_{50} value (µg/ml)			
	Fusarium moniliforme	***Bipolaris oryzae***	***Ustilago hordei***	***Uromyces viciafabia***
Ag_2S-1	13	14	11	14
Ag_2S-2	24	20	10	12
Ag_2S-3	17	15	12	15
Ag_2S-4	11	13	8	11
Ag-NPs	24	27	18	24
*Tilt	25	-	-	-
**Captan	-	35	-	-
***Carboxin	-	-	78	70

*Standard fungicide against *Fusarium moniliforme*

** Standard fungicide against *Bipolaris oryzae*

*** Standard fungicide against *Ustilago hordei* and *Uromyces viciafabia*

Sample Ag_2S-4 exhibited the most significant inhibition of fungal growth against all the test fungi with ED_{50} values 11, 13, 8 and 11µg/ml corresponding to *Fusarium moniliforme, Bipolaris oryzae*, *Ustilago hordei* and *Uromyces viciafabia respectively*. These values were multi-fold lower than the standard fungicides, used against respective fungi.The Ag_2S-NPs were compared with silver nanoparticles (Ag NPs) for their antifungal potential. The results of antifungal activity clearly indicated that Ag_2S-NPs were more effective antifungal agents than Ag NPs against all the four test fungi.

Table 3. Antifungal potential of aqua-dispersed Ag_2S-(1-4) NPs and Ag NPs against *U. hordei*

Sample	Percent inhibition ± standard deviation					Tukey mean test
	5 µg/ml	10 µg/ml	15µg/ml	20 µg/ml	25 µg/ml	
Ag_2S-1	24.63±2.08	47.58±1.52	70.71±3.29	96.01±1.93	100±0.57	59.66[b]
Ag_2S-2	26.34±1.52	52.89±1.15	76.32±1.52	100.00±0.57	100±0.0	70.93[a]
Ag_2S-3	20.79±1.52	38.16±2.64	62.47±2.51	81.52±1.73	100±0.57	61.13[b]
Ag_2S-4	29.13±1.52	58.27±1.52	87.58±1.52	100.00±1.52	100±0.57	75.20[a]
Ag-NPS	15.27±2.51	28.43±1.52	43.15±1.52	55.29±2.08	63.18±1.52	41.13[d]
***Carboxin**	-	-	-	-	12.13±0.53	7.60[e]

*** Standard fungicide against *U. hordei*

Table 4. Antifungal potential of aqua-dispersed Ag_2S-(1-4) NPs and Ag NPs against *U. viciafabia*

Sample	Percent inhibition ± standard deviation					Tukey mean test
	5 µg/ml	10 µg/ml	15µg/ml	20 µg/ml	25 µg/ml	
Ag_2S-1	20.63±1.57	36.58±1.57	52.71±1.52	69.01±1.52	83.56±1.00	53.13[c]
Ag_2S-2	24.34±3.05	39.89±1.52	58.32±1.15	76.00±1.52	89.64±1.52	57.66[b]
Ag_2S-3	16.79±2.00	30.16±3.00	47.47±2.51	59.52±2.08	75.39±1.52	46.33[d]
Ag_2S-4	27.13±1.00	49.27±1.52	65.58±1.00	89.00±1.52	100±0.57	66.06[a]
Ag-NPS	9.11±1.52	21.71±2.08	33.03±2.00	44.21±2.00	53.78±1.52	33.86[e]
***Carboxin**	-	-	-	-	17.65±1.00	32.80[e]

*** Standard fungicide against *U. viciafabia*

Table 5. Antifungal potential of aqua-dispersed Ag_2S-(1-4) NPs against *F. moniliforme*

Sample	Percent inhibition ± standard deviation					Tukey mean test
	5 µg/ml	10 µg/ml	15µg/ml	20 µg/ml	25 µg/ml	
Ag_2S-1	19.39±1.52	39.05±2.00	58.12±1.00	76.48±3.05	95.27±1.57	57.5333[b]
Ag_2S-2	10.21±1.00	22.83±1.00	30.34±1.52	43.39±1.52	58.59±2.00	33.0667d
Ag_2S-3	15.31±2.00	30.59±1.52	45.28±1.00	64.58±3.00	78.19±2.08	47.2000c
Ag_2S-4	23.63±1.73	47.73±2.08	69.08±1.15	96.05±1.52	100.00±0.57	66.8000a
Ag-NPS	08.00±2.08	15.03±2.08	25.13±1.52	38.19±1.52	57.56±0.57	29.4000e
*** Tilt**	-	-	-	-	49.63±1.00	5.3333[f]

*Standard fungicide against *F. moniliforme*

Table 6. Antifungal potential of aqua-dispersed Ag_2S-(1-4) NPs against *B. oryzae*

Sample	Percent inhibition ± standard deviation					Tukey mean test
	5 µg/ml	10 µg/ml	15µg/ml	20 µg/ml	25 µg/ml	
Ag_2S-1	18.12±1.52	32.12±2.00	58.31±1.52	72.79±1.52	93.59±2.00	54.46[b]
Ag_2S-2	13.15±1.52	28.35±1.52	36.75±2.00	55.43±1.52	67.13±1.00	40.66[d]
Ag_2S-3	17.45±2.51	30.98±2.00	47.32±1.52	70.17±1.52	83.56±2.01	50.80[c]
Ag_2S-4	20.38±1.52	39.43±1.52	65.17±1.52	83.05±1.00	100.00±0.57	61.66[a]
Ag-NPS	07.59±2.51	12.58±0.57	23.09±1.52	35.83±1.52	49.00±1.00	26.46[f]
****Captan**	-	-	-	-	37.16±1.00	33.33[e]

** Standard fungicide against *B. oryzae*

Fig. 23Ag_2S-1 @ 20 µg/ml against *F.moniliforme*

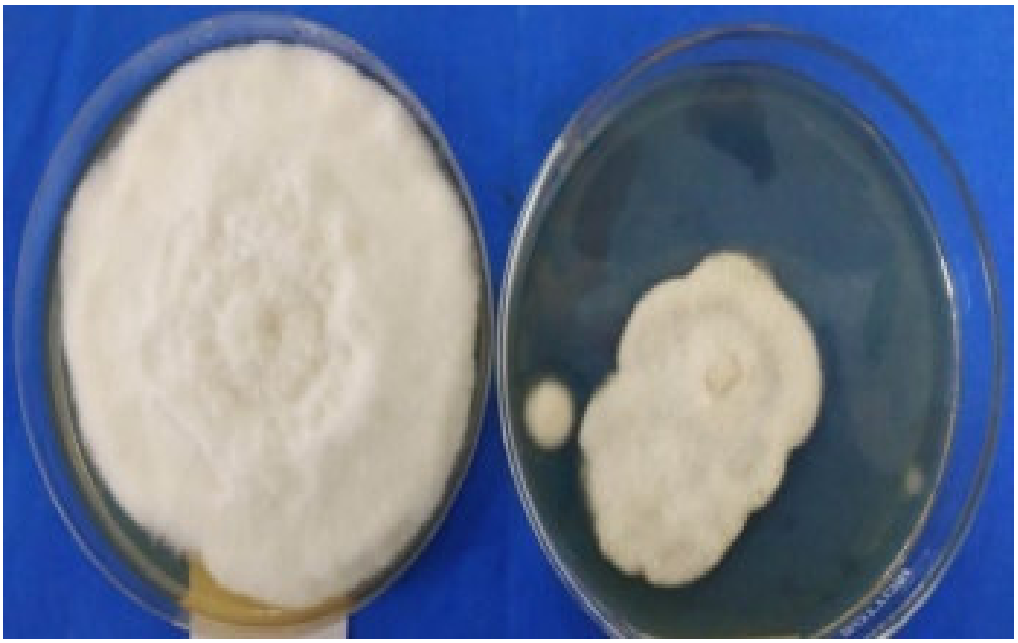

Fig. 24 Ag_2S-2 @ 20 µg/ml against *F.moniliforme*

Fig. 25 Ag_2S-3 @ 20 µg/ml against *F.moniliforme*

Fig. 26 Ag_2S-4 @ 20 µg/ml against *F.moniliforme*

Fig. 27 AgNPs@ 20 µg/ml against *F.moniliforme*

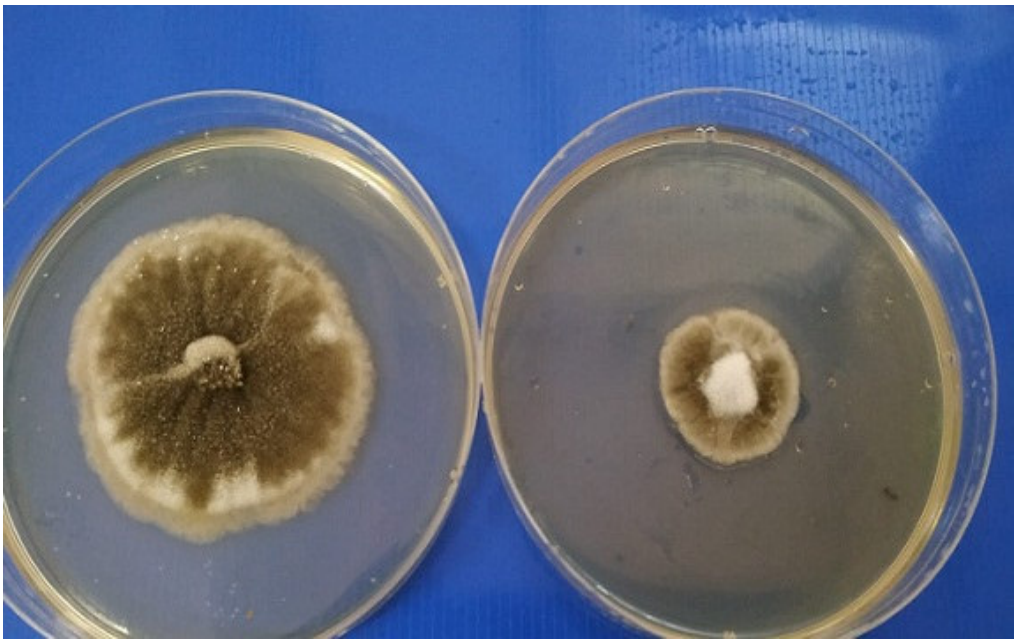

Fig. 28 Ag_2S-1 @ 20 µg/ml against *B. oryzae*

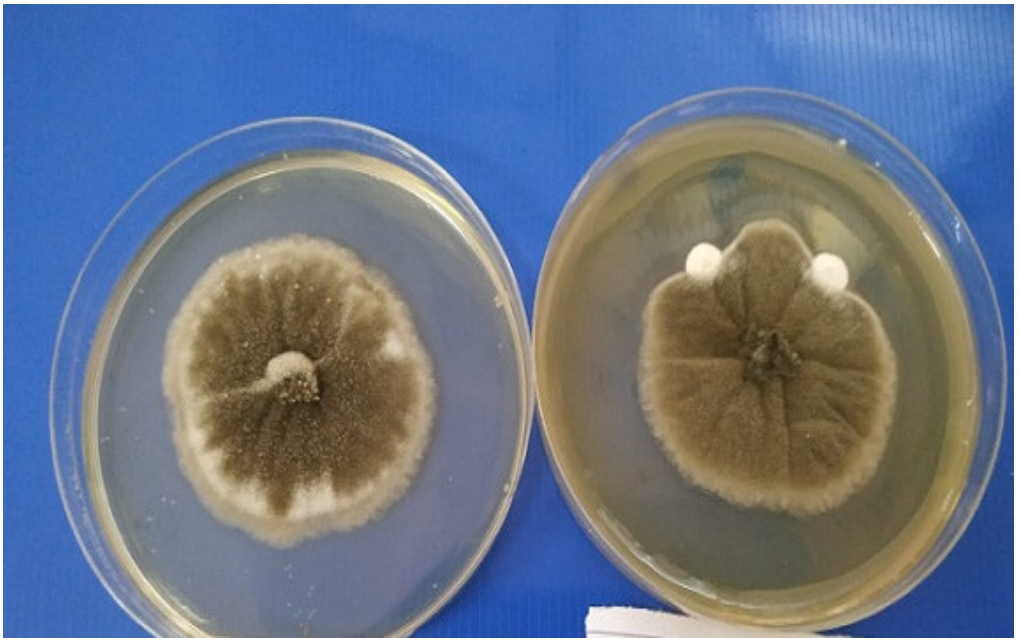

Fig. 29 Ag_2S-2 @ 20 µg/ml against *B. oryzae*

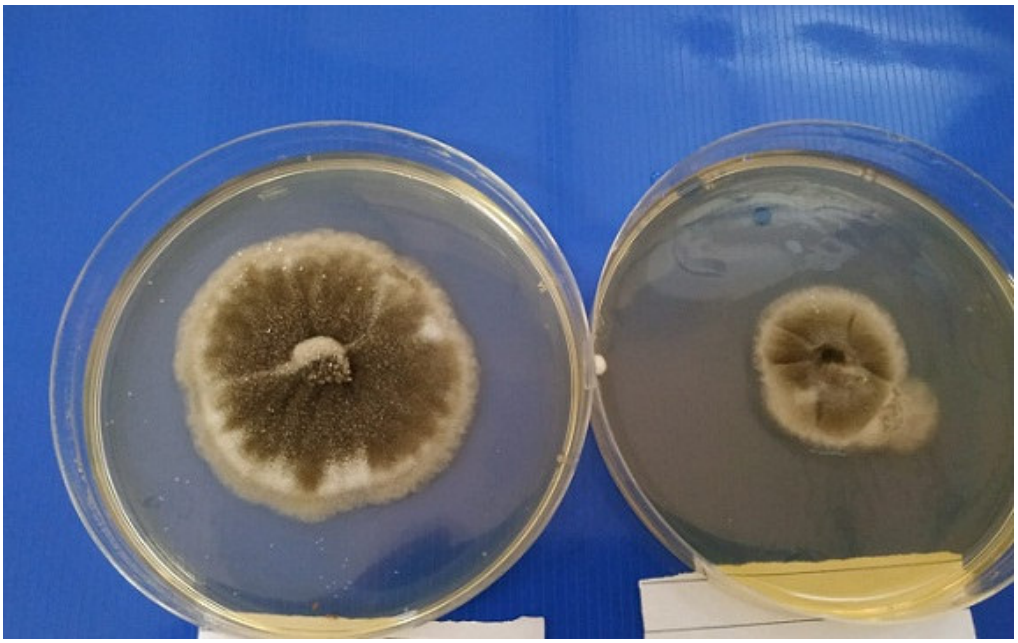

Fig. 30 Ag_2S-3 @ 20 µg/ml against *B. oryzae*

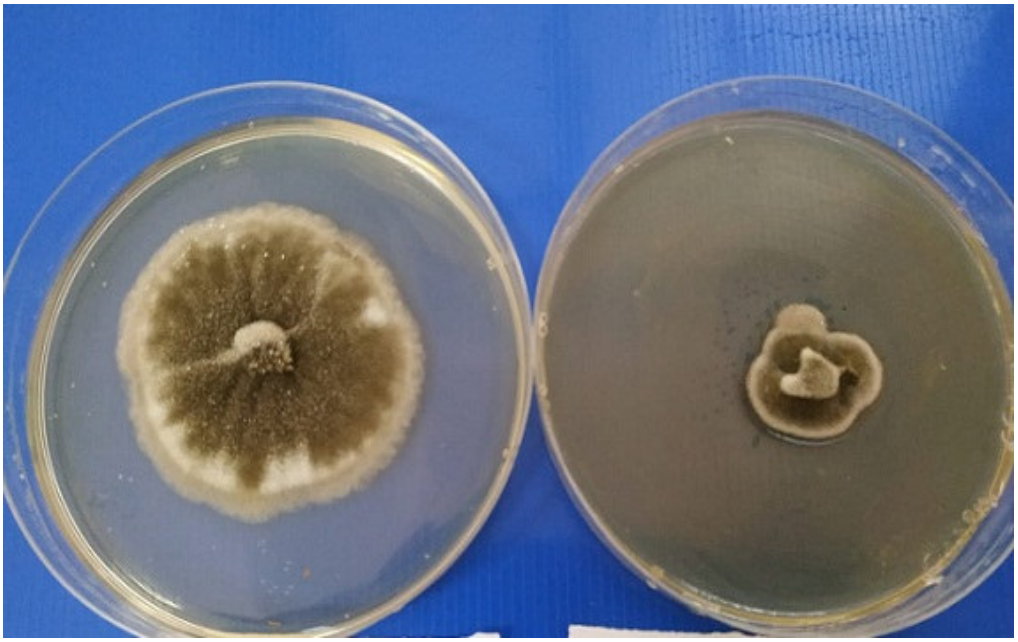

Fig. 31 Ag_2S-4 @ 20µg/ml against *B. oryzae*

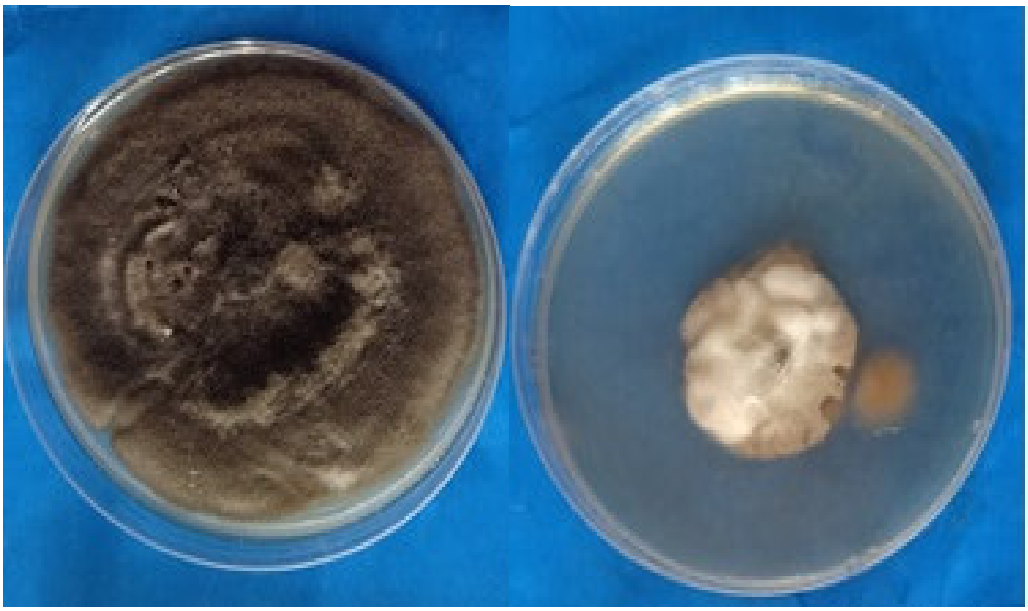

Fig. 32 AgNPs@ 20µg/ml against *B. oryzae*

4.6 Antifungal Activity of Chitosan decorated Ag_2S NPs

The most active sample was further coated with chitosan nanoparticles. The nanoconjugates were screened *in vitro,* against *Fusarium moniliforme, Bipolaris oryzae, Ustilago hordei* and *Uromyces viciafabia*. The antifungal potential of nanoconjugates was compared with the most active sample of Ag_2S NPs i.e. Ag_2S-4 NPs. It was found that the conjugated-compound inflicted less antifungal potential than Ag_2S-4 NPs. There was no synergistic effect of chitosan nanoparticles to enhance the antifungal potential of compound, as ED_{50} value of decorated nanoparticles was very high as compared to Ag_2S-4 NPs (Table 7).

Table 7. Comparison of antifungal potential of Ag_2S-4 NPs with its nanoconjugate

Compound	ED_{50} values (μg ml^{-1})			
	F. moniliforme	***B. oryzae***	***U. hordei***	***U. viciafabia***
Ag_2S-4	11	13	8	11
Ag_2S-C	28	35	25	31

This indicated that Ag_2S NPs interaction with fungal hyphae was the main reason for bioactivity profile. The nanoconjugation masks the Ag_2S nanocore and slows down its release interaction with fungal hyphae and hence lowering the biopotential in case of chitosan coated Ag_2S NPs.

CHAPTER-V

SUMMARY

Silver sulfide nanoparticles (Ag_2S NPs) were synthesized sonochemically using silver nitrate as silver ion source and various sulfide ion sources with Triton –X (a recommended surfactant for antifungal active agents). The prepared samples were characterized by transmission electron microscopy (TEM), UV-Visible spectroscopy (UV-Vis), fourier transform infra-red spectra (FTIR), Dynamic light scattering (DLS), zeta potential, scanning electron microscopy and energy dispersive spectroscopy (SEM-EDS).

The morphology of synthesized Ag_2S NPs in aqua-dispersed form was spherical in nature with particle size varied from 10-20 nm. The maximum absorption between 270-295 nm indicated the presence of Ag_2S NPs. Optical properties of the Ag_2S NPs were measured in freshly prepared dispersions as well as in the same dispersions after regular intervals of 15 days till 4 months. There were no significant diversions from the starting values revealing long shelf life of prepared nano-dispersions. SEM images revealed the nanowired structure of Ag_2S NPs in sample Ag_2S-2 and Ag_2S-3 whereas spherical morphology of the particles was observed in case of sample Ag_2S-1 and Ag_2S-4. EDS spectra confirmed the presence of Ag and S elements in appropriate quantity with no other elemental impurities in all the samples. The hydrodynamic diameter obtained from DLS size distribution of synthesized silver sulfide nanoparticles **Ag_2S-(1-4)** were 224.7 nm, 228.4 nm, 143.74 nm and 113.25 nm respectively. The size obtained from DLS size distribution was much higher than TEM; this was due to the involvement of solvation layer around the particles. The zeta potentials of Ag_2S-1, Ag_2S-2, Ag_2S-3andAg_2S-4 were -14.6 mV, -12 mV, -13.7 mV and -16.2 mV respectively, which confirmed the higher stability of nanoparticles.

Silver nanoparticles were synthesized by means of chemical reduction method, using sodium borohydride as reducing agent. The maximum absorption was absorbed at 412 nm and the average particle size was 8.6-8.8 nm.

All the prepared samples of Ag_2S NPs and Ag NPs were screened for their *in vitro* antifungal potential against various phytopathogenic fungi *viz. Ustilago hordei, Uromyces viciafabia* (spore germination inhibition method), *Fusarium moniliforme* and *Bipolaris oryzae* (PDA method).

Sample Ag_2S-4 exhibited the most significant inhibition of fungal growth against all the test fungi with ED_{50} values 11, 13, 8 and 11 µg/ml corresponding to *Fusarium moniliforme, Bipolaris oryzae, Ustilago hordei* and *Uromyces viciafabia* respectively. These values were multi-fold lower than the standard fungicides, used

against respective fungi.The Ag_2S-NPs were compared with silver nanoparticles (Ag NPs) for their antifungal potential. The results of antifungal activity clearly indicated that Ag_2S-NPs were more effective antifungal agents than Ag NPs against all the four test fungi.

The most active sampleAg_2S-4 was selected for the further conjugation with chitosan NPs (C NPs). Different molar concentrations of Ag_2S NPs and chitosan NPs were tested and 1:2 (C NPs: Ag_2S NPs) was found to be perfect ratio for their conjugation as indicated by TEM image. The nanoconjugation was confirmed by FTIR and TEM analysis of the nanoconjugate, which showed that the chitosan NPs got decorated over the surface of Ag_2S NPs .The conjugated sample was taken for fungicidal potential against pathogenic fungi. It was found that the ED_{50} value of chitosan decorated Ag_2S NPs was very high in comparison to Ag_2S NPs and there was no synergistic effect of chitosan nanoparticles to enhance the antifungal potential of Ag_2S NPs, therefore Ag_2S NPs without conjugation with chitosan nanoparticles can be taken as lead molecule for further studies.

REFRENCES

Aashritha S (2013) Synthesis of silver nanoparticles by chemical reduction method and their antifungal activity. *Int Res J Pharmacy* **4**(10): 111-13.

Agasti N, Singh V K and Kaushik N K (2014) Synthesis of water soluble glycine capped silver nanoparticles and their surface selective interaction. *Mater res Bull* **64**: 17-21.

Akamatsu K, Takeib S, Mizuhata M, Kajinami A, Deki S, Takeokac S, Fujiid M, Hayashid S, and Yamamoto K (1999) Preparation and characterization of polymer thin films containing silver and silver sulfide nanoparticles. *Thin Solid Films* **359**: 55-60.

Aleali H, Mansour N and Mirzaie M (2014) Nonlinear Absorption and Scattering in Wide Band Gap Silver Sulfide Nanoparticles Colloid and Their Effects on the Optical Limiting. *Int J Phys Math Sci* **8**(9): 1274-77.

Almeida J M P, Lu C, Mendonça C R and Arnold C B (2015) Single-step synthesis of silver sulfide nanocrystals in arsenic trisulfide. *Opt Mater Express* **5**: 1815-21.

Anthony S P (2009) Synthesis of Ag_2S and Ag_2Se nanoparticles in self assembled block copolymer micelles and nano-arrays fabrication. *Mater Lett* **63**: 773-76.

Aramwit P, Bang N, Ratanavaraporn J and Ekgasit S (2014) Green synthesis of silk sericin-capped silver nanoparticles and their potent anti-bacterial activity. *NanoscaleRes Lett* **9**(1): 136-47.

Aranaz I, Harris R and Heras A (2010) Chitosan amphiphilic derivatives: chemistry and applications. *Curr Org Chem* **14**: 308-30.

Aranaz I, Mengibar M and Harris R (2009) Functional characterization of chitin and chitosan. *Curr Chem Biol* **3**: 203-30.

Arani M S and Niasari M S (2014) Structural and spectroscopic characterization of prepared Ag_2S nanoparticles with a novel sulfuring agent. *Spectro chim Acta* **133**: 463-71.

Azuma K, Osaki T, Minami T and Okamoto Y (2015) Anticancer and anti-inflammatory properties of chitin and chitosan oligosaccharides. *J Funct Biomater* **6**: 33-49.

BalyakinI A, KuznetsovaY V and Rempel A A (2018) Zeta Potential and Hydrodynamic Radii of Silver SulfideNanoparticles in a Colloidal Solution with Mercaptopropylsilane. *Russ J Phys Chem* **92**(9): 1445-50.

Benhabiles M S, Salah R, Lounici H, Drouiche N, Goosen M F A and Mameri N (2012) Antibacterial activity of chitin, chitosan and its oligomers prepared from shrimp shell waste. *Food Hydrocoll* **29**: 48-56.

Bhata S and Maitra U (2008) Facially amphiphilic thiol capped gold and silver nanoparticles. *J Chem Sci* **120**(6): 507-13.

Brelle M C, Zhang J Z, Nguyen L and Mehra R K (1999) Synthesis and Ultrafast Study of Cysteine and Glutathione-Capped Ag_2S Semiconductor Colloidal Nanoparticles. *J Phys Chem A* **103**: 10194- 201.

Chandra S and Kumar A (2011) Green approach for the synthesis of silver-nanoparticles and efficient use in oxidative cyclization. *Int J App Bio Pharma Tech* **2**(1): 78-85.

Chaudhuri R G and Paria S (2012) A novel method for the templated synthesis of Ag_2S hollow nanospheresin aqueous surfactant media. *J Colloid Interface Sci* **369**: 117-22.

Chen M H and Gao L (2006) Synthesis of leaf-like Ag_2S nanosheets by hydrothermal method in water alcohol homogenous medium. *Mater Lett* **60**: 1059-62.

Chen R, Nuhfer T, Moussa L, Morris H R and Whitmore P M (2008) Silver sulfide nanoparticle assembly obtained by reacting an assembled silvernanoparticle template with hydrogensulfide gas. *Nanotechnol* **19**: 1-11.

Cheng K, Hung Y, Chen C, Liu C and Young J (2014) Green synthesis of chondroitin sulfate-capped silver nanoparticles: Characterization and surface modification. *Carbohydrate Polymers* **110:** 195-202.

Cui C, Li X, Liu J, Hou Y, Zhao Y and Zhong G (2015) Synthesis and functions of Ag_2S nanostructures. *Nanoscale Res Lett* **10**: 1-21.

Das R, Gang S and Nath S S (2011) Preparation and antibacterial activity of silver nanoparticles. *J Biomate Nanobiotech* **2**: 472-75.

Das R, Saha M, Hussain S A and Nath S S (2013) Silver nanoparticles and their antimicrobial activity on a few bacteria. *Bio Nano Sci* **3**(1): 67-72.

Debabov V G, Voeikova T A, Shebanova A S, Shaitan K V, Emelyanova L K, Novikova L M and Kirpichnikov M P (2013) Bacterial synthesis of silver sulfide nanoparticles. *Nanotechnol Russia* **8**: 269-76.

Dehghanipour M, Khanzadeh M, Karimipour M and Molaei M (2017) Dependence of nonlinear optical properties of Ag_2S@ZnS core-shells on Zinc precursor and capping agent. *Opt Laser Technol* **100**: 286-93.

Ding Y, Xu B, Guo R and Shen M (2005) The preparation of silver sulfide nanoparticles in lamellar liquid crystal and application to lubrication. *Mater Res Bull* **40:** 575-82.

Dini L, Panzarini E, Serra A, Buccolieri A and Manno D (2011) Synthesis and in vitro cytotoxicity of glycans-capped silver nanoparticles. *Nanomater nanotechnol* **1**(1): 58-64.

Dong L, Chu Y, Liu Y and Li L (2008) Synthesis of faceted and cubic Ag_2S nanocrystals in aqueous solutions. *J Coll Interface Sci* **317**: 485-92.

Ebrahiminezhad A, Raee M J, Manafi Z, Jahromi A S and Ghasemi Y (2016) Ancient and novel forms of silver in medicine and biomedicine. *J Adv Med Sci Appl Technol (JAMSAT)* **2**:122-28.

Elgorbana A M, El-Samawatya A E M, Yassin M A, Sayed S R, Adile S F, Elhindif K M, Bakrig M and Khane M (2016) Antifungal silver nanoparticles: synthesis, characterization and biological evaluation. *Biotech Biotechnolog Equip* **30**(1): 5662.

Emadi H, Niasari M S and Davar F (2011) Synthesis and characterization of silver sulfide nanoparticles by ultrasonic method. *Micro Nano Lett* **6**: 909-13.

Ezenwa I A, Okereke N A and Egwunyenga N J (2012) Optical Properties of Chemical Bath Deposited Ag_2S Thin Films. *Int J Sci Tech* **2**: 224-3577.

Fakhri A, Pourm M, Khakpour R and Behrouz S (2015) Structural, optical, photoluminescence and antibacterial properties of copper-doped silver sulfide nanoparticles. *J Photochem Photobiol B* **149**: 78-83.

Fang Y, Bai C and Zhang Y (2004) Preparation of metal sulfide–polymer composite microspheres with patterned surface structures. *Chem Commun* **2004**: 804-05.

Farasat M and Golzan M M (2014) Preparation and characterization of methyltrimethoxysilane-Ag nanoparticles using chemical reduction at room temperature. *Appl Nanosci* **4**: 293-97.

Friedman A J, Phan J and Schairer D O (2013) Antimicrobial and anti-inflammatory activity of chitosan- alginate nanoparticles: a targeted therapy for cutaneous pathogens. *J Invest Dermatol* **133**: 1231-39.

Guo L, Panderi I, Yan D D, Szulak K, Li Y, Chen Y, Ma H, Niesen D B, Seeram N, Ahmed A, Yan B, Pantazatos D and Lu W (2013) A comparative study of hollow copper sulfide nanoparticles and hollow gold nanosphere on degradability and toxicity. *ACA Nano* **7**:8780–93.

Guzman M G, Dille J and Godet S (2009) Synthesis of silver nanoparticles by chemical reduction method and their antibacterial activity. *Int J Chem Biomol Engg* **2**(3): 104-11.

Han L, Lv Y, Asiri A M, Al-Youbi A O, Tu B and Zhao D (2012) Novel preparation and near-infrared photoluminescence of uniform core-shell silver sulfide nanoparticle@mesoporous silica nanospheres. *J Mater Chem* **22**: 7274-79.

Hashmi L (2010) Synthesis and characterization of silversulfide nanoparticles of various morphologies using chitosan as stabilizer.(ed) *AIP Conference.* Vol. **1276** pp 62-69, American Institute Physics.

Hebeish A, Shaheen T I and El-Naggar M E (2016) Solid state synthesis of starch-capped silver nanoparticles. *Int J Biol Macromol* **87**:70-76.

Ismail M, Yuri M, Farit U, Ahmed A I S, Muhambetkali B and Bolat U (2016) Antifungal activity of inorganic micro and nanoparticles against pathogenic fungi compared with some traditional organic drugs. *American-Eurasian J Agric & Environ Sci* **16**: 652-62.

Jang K, Kim S Y, Park K H, Jang E, Jun S and Son S U (2007) Shape-controlled synthesis of silver sulfide nanocrystals through the understanding of the origin of the mixed-shape evolution. *Elect supplem inform* **2017**: 1-5.

Jin H, Gui R, Gong J and Huang W (2016) Aptamer and 5-fluorouracil dual-loading Ag_2S quantum dots used as asensitive label-free probe for near-infrared photoluminescence turn-on detection of CA125 antigen. *Biosens Bioelectron* **92:** 378-84.

Jung E J, Youn D K, Lee S H, No H K, Ha J G and Prinyawiwatkul W (2010) Antibacterial activity of chitosan with different degrees of deacetylation and viscosities. *Int J Food Sci Technol* **45**: 676-82.

Karimipour M, Moradi N, Molaei M (2016) Strong NIR luminescent Ag_2S@ZnS core-shells synthesized by a novel one pot pulsed microwave irradiation. *J Lumin* doi.org/10.1016/j.jlumin.2016.09.063.

Kasture M B, Patel P, Prabhune A A, Ramana C V, Kulkarni A A and Prasad B L V (2008) Synthesis of silver nanoparticles by sophorolipids: Effect of temperature and sophorolipid structure on the size of particles. *J Chem Sci* **120**(6): 515-20.

Kim B, Park C S, Murayama M and Hochella M F (2009) Discovery and Characterization of Silver Sulfide Nanoparticles in Final Sewage Sludge Products. *Environ Sci Technol* **44**: 7509-14.

Kim S W, JungJ H, Lamsal K, Kim Y S, Min J S and LeeY S (2012)Antifungal Effects of Silver Nanoparticles (AgNPs) against various plant pathogenic fungi. *Mycobiology* **40**(1): 53-58.

Kim Y and Walsh D (2010) Metal sulfide nanoparticles synthesized via enzyme treatment of biopolymer stabilized nanosuspensions. *Nanoscale* **2**: 240-47.

Kora A J and Rastogi L (2013) Enhancement of antibacterial activity of capped silver nanoparticles in combination with antibiotics, on model Gram-Negative and Gram-Positive bacteria. *Bioinorg Chem App* **13**: 1-7.

Krishnaraj C, Ramachandran R and Mohan K (2012) Optimization for rapid synthesis of silver nanoparticles and its effect on phytopathogenic fungi. *Spectrochim Acta A Mol Biomol Spectrosc* **93**: 95- 99.

Kristl M, Gyergyek S, and Kristl J (2015) Synthesis and characterization of nanosized silver chalcogenides under ultrasonic irradiation. *Mater Express* **5**: 359-66.

Kubie L, King L A, Kern M E, Murphy J R, Kattel S ,Yang Q, Stecher J T, Rice W D and Parkinson B A (2017) Synthesis and Characterization of Ultrathin Silver Sulfide Nanoplatelets. *ACS Nano* **11**: 8471-77.

Kumar B, Smita K, Cumbal L, Debut A, Camacho J, Hernández-Gallegos E, Chavez-Lopez M G, Grijalva M, Angulo Y and Rosero G (2015) Pomosynthesis and biological activity of silver nanoparticles using *Passiflora tripartita* fruit extracts. *Adv Mater Lett* **6**: 127-32.

Kumari P, Chandran P and Khan S K (2014) Synthesis and characterization of silver sulfide nanoparticles for photocatalytic and antimicrobial applications. *J Photochem Photobio B: Biology* **141**: 235–40.

Kuznetsovaa Y V, Rempela S V, Popova I D, Gerasimovc E Y and Rempela A A (2017) Stabilization of Ag_2S nanoparticles in aqueous solution by MPS. *Colloids and Surfaces A: Physicochem Eng Aspects* **520**: 369-77.

Leo´n-Vela´zquez M S, Irizarry R and Castro-Rosario E M (2010) Nucleation and growth of silver sulfide nanoparticles. *J Phy Chem C* **114**: 5839–49.

Li X, Zhang J, Xu W, Jia H, Wang X, Yang B, Zhao B, Li B and Ozaki Y (2003) Mercaptoacetic acid-capped silver nanoparticles colloid: formation, morphology and SERS activity. *American Chem Soc* **19**(10): 4285-90.

Lim W P, Zhang Z, Low H Y and Chin W S (2004) Preparation of Ag_2S Nanocrystals of Predictable Shape and Size. *Angew Chem Int Ed* **43:** 5685-89.

Liu H, Ye F, Cao H, Ji G, Lee J Y and Yang J (2013) A core–shell templated approach to the nanocomposites of silver sulfide and noble metal nanoparticles with hollow/cage-bell structures. *Nanoscale* **2013**: 1-7.

Liu M, Xu Z, Li B, Lin C, Bai D, Shan N and You W (2011) Synthesis of worm-like Ag2S nanocrystals in W/O reverse microemulsion. *Mater Lett* **65**: 555–58.

Liu N, Chen X G and Park H J (2006) Effect of MW and concentration of chitosan on antibacterial activity of Escherichia coli. *Carbohydr Polym* **64**: 60-65.

Lv L and Wang H (2014) Ag_2S nanorice: Hydrothermal synthesis and characterization study. *Mater Lett* **121:** 105-08.

MahdizadehV, Safaie N and Khelghatibana F (2015) Evaluation of antifungal activity of silver nanoparticles against some phytopathogenic fungi and *Trichoderma harzianum. J Crop Prot* **4**(3): 291-300.

Malina D, Kupiec A S, Wzorek Z and Kowalski Z (2012) Silver nanoparticles synthesis with different concentrations of polyvinylpyrrolidone. *Digest J Nanomat Biostructures* **7**(4): 1527-34.

Mallmann J J E, Cunha A F, Castro M N, Maciel M A, Menezes E A and Fechine P B A (2015) Antifungal activity of silver nanoparticles obtained by green synthesis. *Rev Inst Med Tro Sao Paulo* **57**(2): 165-67.

Mandal A, Meda V, Zhang W J, Farhan K M and Gnanamani A (2013) Synthesis, characterization and comparison of antimicrobial activity of PEG/TritonX-100 capped silver nanoparticles on collagen scaffold. *Colloids Surf B Biointerfaces* **101**(1): 517-18.

Martinez-Castano G A, Sanchez-Loredo M G, Dorantes H J , Martinez-Mendoza J R and Ortega-Zarzosa G R F (2004) Characterization of silver sulfide nanoparticles synthesized by a simple precipitation method. *Mater Lett* **59**: 529-34.

Mishra S, Singh B R, Singh, Keswani C, Naqvi A H and Singh H B (2014) Biofabricated silver nanoparticles act as a strong fungicide against *Bipolarissorokiniana* causing spot blotch disease inwheat. *PLoS One* **9**: doi.org/10.1371/journal.pone.0097881.

Murugadoss G, Jayavel R, Kumar M R and Thangamuthu R (2015) Synthesis, optical, photocatalytic, and electrochemical studies on Ag_2S/ZnS and ZnS/Ag_2S nanocomposites. *Appl Nanosci* **6**: 503–10.

Nasrollahi A, Pourshamsian K and Mansourkiaee P (2011) Antifungal activity of silver nanoparticles on some of fungi. *Int J Nano Dim* **1**(3): 233-39.

Nath S K and Kalita P K (2012) Chemical synthesis of copper sulfide nanoparticles embedded in PVA matrix. *Nanosci Nanotechnol Inter* **2**: 8**-**12.

Naz S S, Shah M R, Islam N U, Khan A, Nazir S, Qaisar S and Alam S S (2014) Synthesis and bioactivities of silver nanoparticles capped with 5-Amino-β-resorcylic acid hydrochloride dehydrate. *J Nanobiotech* **12**: 34-38.

Ng C K, Sivakumar K, Liu X, Madhaiyan M, Ji L,Yang L,Tang C, Song H, Kjelleberg S and Cao B (2013) Influence of outer membrane c-type cytochromes on particle size and activity of extracellular nanoparticles produced by *Shewanella oneidensis*. *Biotechnol Bioeng* **110**: 1831**-**37.

Oliveira M I, Santos S G, Oliveira M J, Torres A L and Barbosa M A (2012) Chitosan drives anti- inflammatory macrophage polarisation and pro-inflammatory dendritic cell stimulation. *Eur Cell Mater* **24**: 136-53.

Ong W L and Ho G W (2016) Enhanced Photocatalytic Performance of TiO_2 Hierarchical Spheres Decorated with Ag_2S Nanoparticles. *Proc Eng* **141:** 7-14.

Park J K, Chung M J, Choi H N and Park Y I (2011) Effects of the molecular weight and the degree of deacetylation of chitosan oligosaccharides on antitumor activity. *Int J Mol Sci* **12**: 266-77.

Patil R S, Kokate M R, Jambhale C L, PawarS M, Hand H S and Kolekar S S (2012) One-pot synthesis of PVA-capped silver nanoparticles their characterization and biomedical application. *Adv Nat Sci: Nanosci Nanotechnol* **3:** 15-23.

Pileni M P, Motte L, Billoudet F, Mahrt J and Willig F (1996) Nanosized silver sulfide particles: characterization, self-organization into 2D and 3D superlattices. *Mater Lett* **31**: 255-60.

Sadovnikov S I and Gusev A I (2016) Universal Approach to the Synthesis of Silver Sulfide in the Formsof Nanopowders, Quantum Dots, Core-Shell Nanoparticles and Heteronanostructures. *Eur J Inorg Chem* **2016:** 4944-57.

Sadovnikov S I, Gusev A I and Rempel A A (2015) Nanocrystalline silver sulfide Ag2S. *Rev Adv Mater Sci* **41**:7**-**19.

Sadovnikov S I, Kuznetsova Y V and Rempel A A (2016) Ag2S silver sulfide nanoparticles and colloidal solutions: Synthesisand properties**.** *Nanostruct nano objects* **7**: 81**-**91.

Saha S, Gupta B, Gupta K and Chaudhuri M G (2016) Production of putrescine-capped stable silver nanoparticle: its characterization and antibacterial activity against multidrug-resistant bacterial strains. *Appl Nanosci* **16:** 528-29.

Schaaff T G and Rodinone A J (2003) Preparation and Characterization of silver sulfide nanocrystals generated from silver (i)-thiolate polymers. *J Phys Chem B* **107**: 10416**-**22.

Shebanova A S, Voeikova T A, Egorov A V, Novikova L M, Krestyanova I N, Emelyanova L K, Debabov V G, Kirpichnikov M P and Shaytan K V (2014) Study of some aspects of the mechanism of bacterial synthesis of silver sulfide nanoparticles by metal reducing bacteria *Shewanella oneidensis* MR-1. *Cell Biophys* **59**: 408**-**14.

Shukla S, Seal S and Mishra S R (2002) Synthesis and characterization of silver sulfide nanoparticles containing sol-gel derived HPC-silica film for ion-selective electrode application. *J Sol-Gel Sci Technol* **23**: 151-64.

Sibiya N P, Xaba T and Moloto M J (2016) Green synthetic approach for starch capped silver nanoparticles and their antibacterial activity. *Pure Appl Chem* **88**(1): 61-69.

Sidhu A, Barmota H and Bala A (2017) Antifungal evaluation studies of copper sulfide nano- aquaformulations and its impact on seed quality of rice (*Oryzae sativa*). *Appl Nanosci* **7**: 681-89.

Sun Y and Zhou B (2010) Single-crystalline Ag_2S hollow nanohexagons and their assembly into orderedarrays. *Mater Lett* **64**: 1347-49.

Sundar B S, Sarada R, Jagannadharao V and Padma M (2016) Synthesis of 5-Methyl 2-mercapto benzimidazole capped silver nanoparticles via chemical reduction method & study of their biological properties. *The Experiment* **35**(1): 2162-70.

Suresh A K, Doktycz M J, Wang W, Moon J W, Gu B, Meyer H M, Hensley D K, Allison D P,PhelpsT J and Pelletier D A (2011) Monodispersed biocompatible silver sulfide nanoparticles: Facile extracellular biosynthesis using the c-proteobacterium, Shewanella oneidensis. *Acta Biomater***7**: 4253-58.

Takahashi T, Imai M, Suzuki I and Sawai J (2008) Growth inhibitory effect on bacteria of chitosan membranes regulated with deacetylation degree. *Biochem Eng J* **40**:485-91.

Tan C S, Hsiao C H, Wang C S, Liu P H, Lu M Y, Huang M H, Ouyang H and Chen L H (2014) Sequential Cation Exchange Generated Superlattice Nanowires Forming Multiple p-nHeterojunctions. *ACS Nano* **8**: 9422-26.

Tang Q, Yoon S M, Yang H J, Lee Y, Song H J, Byon H R and Choi H C (2005) Selective Degradationof Chemical Bonds: from Single-Source Molecular Precursors to Metallic Ag and Semiconducting Ag_2S Nanocrystals via Instant Thermal Activation. *Langmuir* **22**: 2802-05.

Tiwari V, Khokar M K, Tiwari M, Barala S and Kumar M (2014) Anti-bacterial activity of polyvinylpyrrolidone capped silver nanoparticles on the carbapenem resistant strain of *Acinetobacter baumannii*. *J Nanomed Nanotechnol* **5**(6): 246-52.

Toh H S, Mcauley C B, Tschulik K and Compton R G (2014) Chemical interactions between silvernanoparticles and thiols: a comparison of mercaptohexanol against cysteine. *Sci China Chem* **57**(9): 1199-1210.

Tran Q H, Nguyen V Q and Le A T (2013) Silver nanoparticles: Synthesis, properties, toxicology, applications and perspectives. *Adv Nat Sci: Nanosci Nanotechnol* **4**: 1-20.

Varghese V M, Dhumal R S, Patil S S, Paradkar A R and Khanna P K (2009) Synthesis and In-vitro antimycobacterial studies of cysteine capped silver nano-particles. *Metal OrgNano Met Chem* **39**: 554-58.

Vasireddy R, Paul R and Mitra A K (2012) Green synthesis of silver nanoparticles and the study of optical properties. *Nanomater Nanotechnol* **2**:1-6.

Verma S K, Singh D K, Pandey D K and Yadav R R (2013) Study of nanostructured silver sulfide and its nanofluid. *Natl Acad Sci Lett* **36**: 535-40.

Wang D S, Hao C H, Zhong W, Peng Q, Wang T H, Liao Z M, Yu D P and Li Y D (2008) Ultralong single-crystalline Ag_2S nanowires: promising candidates for photoswitches and room-temperature oxygen sensors. *Adv Mater* **20**: 2628-32.

Wang M, Min Y and Chen Y (2008) Simple approach to NiS_2/Ag_2S composites and their optical properties. *Mater Lett* **62**: 3280-83.

Wang P, Menzies N W, Lombi E, Sekine R, Blamey F P C, Hernandez-Soriano M C, Cheng M, Kappen P, Peijnenburg W J G M, Tang C and Kopittke P M (2015) Silver sulfide nanoparticles (Ag_2S-NPs) are taken up by plants and are phytotoxic. *Nanotoxicol* **9**: 1-9.

Wang T X, Xiao H and Zhang Y C (2008) Simple solid state synthesis of Ag_2S crystallites using a single-source molecular precursor. *Mater Lett* **62**: 3736-38.

Wang W, Chen X and Efrima S (1999) Silver nanoparticles capped by long-chain unsaturated carboxylates. *J Phys Chem B* **103** (34): 7238-46.

Wang X B, Liu W M, Hao J C, Fu X G and Xu B S (2005) A simple large-scale synthesis of well-defined silver sulfide semiconductor nanoparticles with adjustable size. *Chem Lett* **43**:1664-65.

Wang X, Zhuang J, Peng Q and Li Y D (2005) A general strategy for nanocrystal synthesis. *Nature* **437:** 121-24.

Wang Z, Bussche AV D, Kabadi P K, Kane A B and Hurt R H (2013) Biological and environmental transformation of copper-based nanomaterials. *ACS Nano***7**: 8715–27.

Wen X, Wang S, Xie Y, Li X Y and Yang S (2005) Low-Temperature Synthesis of Single Crystalline Ag_2S Nanowires on Silver Substrates. *J Phys Chem B* **109**: 10100-106.

Wu M, Pan X, Qian X, Yin J and Zhu Z (2004) Solution-phase synthesis of Ag_2S hollow and concave nanocubes. *Inorg Chem Commun* **7**: 359-62.

Xaba T, Moloto M J, Nchoe O B, Nate Z and Moloto N (2017) Synthesis of silver sulfide nanoparticles through homogeneous precipitation route and the preparation of the Ag_2S-chitosan nanocomposites for the removal of iron(ii) ion from wastewater. *Chalcogenide Lett* **14**: 337-46.

Xiaodong Z, Huaqiang S, Daming H, Shumin J, Xun F and Kui J (2008) Room temperature synthesis and electrochemical application of imidazoline surfactant-modified Ag2S nanocrystals. *Mater Lett* **62**: 2407-10.

Xu C, Zhang Z, Ye Q (2004) A novel facile method to metal sulfide (metal=Cd, Ag, Hg) nanocrystallite. *Mater Lett* **58**: 1671-76.

Xu Y, Wen Z and Xu Z (2010) Chitosan nanoparticles inhibit the growth of human hepatocellular carcinoma xenografts through an antiangiogenic mechanism. *Anticancer Res* **30**: 5103-10.

Yadav S K and Jeevanandam P (2015) Synthesis of Ag_2S-TiO_2 Nanocomposites and Their Catalytic Activity towards Rhodamine B Photodegradation. *J Alloys Compd* **649**: 483-90.

Yaghmour S J and Mahmoud W E (2013) Synthesis and characterization of self-assembly silver sulfidenanorods prepared by squalene assisted microwave technique. *Mater Lett* **109**: 55-57.

Yan D, He Y, Ge Y and Song G (2011) Fluorescence "turn on-off" detection of heparin and heparinase Ibased on the near-infrared emission polyethyleneimine capped Ag_2S quantum dots. *Mater Lett* **27**: 1-12.

Yan Y, Chen K, Li H, Hong W, Hu X and Xu Z (2014) Capping effect of reducing agents and surfactants in synthesizing silver nanoplates. *Trans Nonferrous Met Soc China* **24**: 3732-38.

Yang G, Lin Q, Wang C, Li J, Wang J, Zhou J, Wang Y and Wang C (2012) Synthesis and characterization of dextran-capped silver nanoparticles with enhanced antibacterial activity. *J Nanosci Nanotechnol* **12**(5): 3766-74.

Yang L, Xing R, Shen Q, Jiang K, Ye F, Wang J and Ren Q (2006) Fabrication of Protein-Conjugated Silver Sulfide Nanorods in the Bovine Serum Albumin Solution. *J Phys Chem B* **110**: 10534-39.

Yang W, Xie T, Jiang T and Wang D (2013) Facile preparation of Ag_2S nanoparticles with broad photoelectric response region. *Colloids Surf A* **433**: 55-58.

Yeo S Y, Tan W L, Bakar M A and Ismail J (2010) Silver sulfide/poly(3-hydroxybutyrate) nanocomposites: Thermal stability and kinetic analysis of thermal degradation. *Polym DegradStab* **95**: 1299-1304.

Younes I and Rinaudo M (2015) Chitin and chitosan preparation from marine sources: structure, properties and applications. *Mar Drugs* **13**: 1133-74.

Younes I, Sellimi S, Rinaudo M, Jellouli M and Nasri M (2014) Influence of acetylation degree and molecular weight of homogeneous chitosans on antibacterial and antifungal activities. *Int J Food Microbiol* **185**: 57-63.

Zhai H J and Wang H S (2007) Ag_2S morphology controllable via simple template-free solution route. *Mater Res Bull* **43**: 2354-60.

Zhang C, Zhang S, Yu L, Zhang Z, Zhang P and Wu Z (2012) Size-controlled synthesis of monodisperse Ag_2S nanoparticles by a solventless thermolytic method. *Mater Lett* **85**: 77-80.

Zhang W, Zhang L, Hui Z, Zhang X and Qian Y (2000) Synthesis of nanocrystalline Ag_2S in aqueous solution. *Solid State Ionics* **130**: 111-14.

Zhang Z, Lim W P, Wong C T, Xu H, Yin F and Chin W S (2012) From metal thiobenzoates to metal sulfide nanocrystals: An experimental and theoretical investigation. *Nanomater* **2**: 113-33.

Zhao Y, Zhang D, Shi W and Wang F (2007) A gamma-ray irradiation reduction route to prepare rod-like Ag_2S nanocrystallines at room temperature. *Mater Lett* **61**: 3232-34.

Zhuang Z, Peng Q, Wang X and Li Y (2007) Tetrahedral colloidal crystals of Ag_2S nanocrystals. *Angew Chem Int Ed* **46**: 8174-77.

ANNEXURE

a)

b)

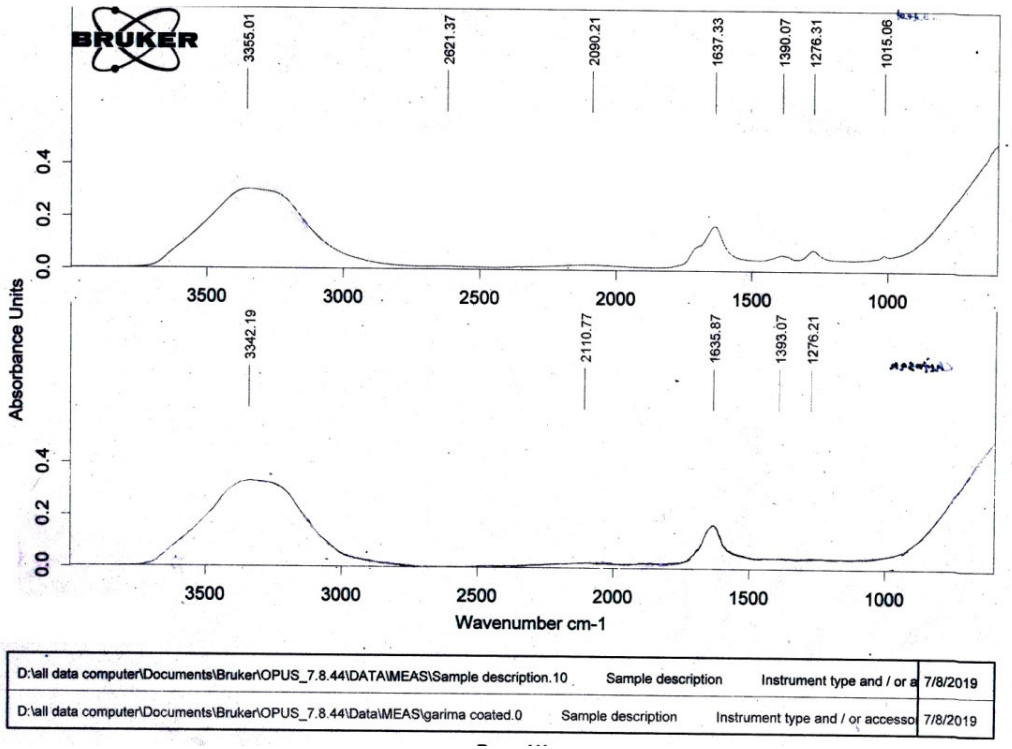

FTIR Spectra of (a) Chitosan decorated Ag_2S NPs and (b) Chitosan

VITA

Name	**:**	Garima Sethi
Father's Name	**:**	Mr. Varinder Sethi
Mother's Name	**:**	Mrs. Renu Sethi
Nationality	**:**	Indian
Date of Birth	**:**	15th December 1996
Permanent Address	**:**	St. No. 7, Badi Pouri, Nai Abadi, Abohar, Fazilka-152116, Punjab, India

EDUCATIONAL QUALIFICATION

Bachelor's Degree	**:**	B.Sc. (Hons.) Chemistry
University	**:**	DAV University, Jalandhar
Year of award	**:**	2017
OCPA	**:**	8.63/10.00
Master's Degree	**:**	M.Sc.
University	**:**	Punjab Agricultural University, Ludhiana
Year of Award	**:**	2019
OCPA	**:**	8.00/10.00
Title of Master's Thesis	**:**	"Synthesis of surface modified silver sulfide nanoparticles as antifungal agents"